Palestine Polytechnic University

Deanship of Graduate Studies and Scientific Research

Master of Civil Engineering

Pushover Analysis of Seismic Performance for Steel Trusses Bridges

Student Name:
Wael Abu Jame'

Supervisor:
Dr. Belal Almassri

Thesis submitted in partial fulfillment of requirements of the degree
Master of Civil Engineering

May, 2023

The undersigned hereby certify that they have read, examined and recommended to the Deanship of Graduate Studies and Scientific Research at Palestine Polytechnic University:

Pushover Analysis of Seismic Performance for Steel Trusses Bridges

Student Name: Wael Abu Jame'

in partial fulfillment of the requirements for the degree of Master in Civil Engineering:

Graduate Advisory Committee:

Assistant Prof./Dr Belal Almassri (Supervisor), Palestine Polytechnic University

Signature:———————————— Date:————————————

Associate Prof./ Dr Yousri Sweity (External committee member), Tver state of technical university, Russia

Signature:———————————— Date:————————————

Assistant Prof./Dr Maher Amro (Internal committee member), Palestine Polytechnic University

Signature:———————————— Date:————————————

Thesis Approved by:

Name:

Dean of Graduate Studies & Scientific Research

Palestine Polytechnic University

Signature:……...……

Date:…..……...……

Pushover Analysis of Seismic Performance for Steel Trusses Bridges

Student Name: Wael Abu Jame'

ABSTRACT

Pushover analysis has become an effective tool for seismic design of medium and high-rise buildings under dynamic loads and severe earthquakes. However, in order to apply a traditional pushover analysis can be difficult for complicated steel structures such as large span structures. In this research, pushover analysis was adopted to evaluate the dynamic behavior of some steel truss structures under severe dynamic loads and earthquakes. Results and discussions are presented for some case studies of previous collapsed steel truss and long span bridges. Pushover curves will be obtained by nonlinear static analysis. The maximum displacements and plastic hinge positions will be located by pushover analysis, the main objective of this master research thesis is to review previous failure mechanisms of previous steel trusses structures/bridges, moreover check the possibility of assessing steel truss structures using pushover analysis using parametric study in order to check some important structural aspects.

تقييم الأداء الزلزالي للجسور الفولاذية باستخدام طريقة التحليل الزلزالي الاستاتيكي اللاخطي

اسم الطالب: وائل أبو جامع

الملخص

أصبحت طريقة التحليل الزلزالي اللاخطي الاستاتيكي أداة فعالة للتصميم الزلزالي للمباني المتوسطة والشاهقة تحت الأحمال الديناميكية والزلازل الشديدة. ومع ذلك ، من أجل تطبيق تحليل انسيابي تقليدي ، قد يكون من الصعب على الطرق التحليلة توقع تصرف الهياكل الفولاذية المعقدة مثل الهياكل ذات الطول الكبير. في هذا البحث تم اعتماد التحليل اللاخطي لتقييم السلوك الديناميكي لبعض هياكل الجمالونات الفولاذية تحت الأحمال الديناميكية الشديدة والزلازل. سيتم عرض النتائج لبعض دراسات الحالة الخاصة بالجمالونات الفولاذية المنهارة والجسور الطويلة. سيتم الحصول على منحنيات طريقة التحليل الزلزالي اللاخطي. سيتم تحديد الحد الأقصى للإزاحة ومواضع الانهيار والعقد البلاستيكية، والهدف الرئيسي من هذه الأطروحة البحثية هو مراجعة آليات الفشل السابقة لجسور فولاذية ، علاوة على ذلك التحقق من إمكانية تقييم هياكل الجمالون الفولاذية باستخدام طريقة دراسة العوامل المؤثرة على النتائج مثل قوة خضوع الحديد بالاضافة الى طول الجسور وعدد الركائز.

DECLARATION

I declare that the Master Thesis entitled" **Pushover Analysis of Seismic Performance for Steel Trusses Bridges**" is my own original work, and herby certify that unless stated, all work contained within this thesis is my own independent research and has not been submitted for the award of any other degree at any institution, except where due acknowledgement is made in the text.

Student Name: **Wael Abu Jame'**

Signature:———————————— Date:————————————

DEDICATION

I would like to dedicate this thesis to my family. Thank you so much for everything! Words can hardly describe my thanks and appreciation to you. You have been my source of inspiration, support, and guidance. You have taught me to be unique, determined, to believe in myself, and to always persevere. I am truly thankful and honored to have you as my wife.

Special thanks to my colleagues and everyone helped me to accomplish this research, especially to my beloved teachers at Palestine Polytechnic University.

To my family and friends,

I dedicate this humble work.

ACKNOWLEDGEMENT

I would like to express my sincere gratitude to my advisor, **Dr. Belal Almassri**, the head of civil engineering department for his invaluable guidance and support throughout my master's program. His expertise and encouragement helped me to complete this research and write this thesis.

I would also like to thank **Dr. Maher Amro and Dr. Haitham Ayyad** for their efforts at the master program of civil engineering. I am also grateful to **Palestine Polytechnic University** for providing me with the opportunity to conduct my research and for all of the resources and support they provided.

I would also like to thank **my friends and family** for their love and support during this process. Without them, this journey would not have been possible.

Special thanks to the external committee member **Dr Yousri Sweity.**

Finally, I would like to thank all of the participants in my study for their time and willingness to share their experiences. This work would not have been possible without their contribution.

List of Abbreviations

RSM: Response Spectrum Method

NTHA: Nonlinear time history analysis

PA: Pushover Analysis

AASHTO: American Association of State Highway and Transportation Officials

ASCE: American Society of Civil Engineers

LRFD: Load and Resistance Factor for Design

UBC: Uniform Building Code

PGA: Peak Ground Acceleration

SA: Spectral Acceleration

FHWA: Federal Highways Administration

SFRS: Seismic Force Resistance System

IBC: International Building Code

MSSS: Multispan simply supported

MSC: Multispan continuous

CSUS: steel girder bridges in the central and southeastern United

ATC: Applied technology council

NSP: Nonlinear static procedure

NYSDOT: The New York State Department of Transportation

PSHA: Probabilistic seismic hazard analysis

FEM: Finite Element Modelling

List of Figures

List of Tables

Table of Contents

Chapter 1: Introduction

1.1 General Introduction

Steel truss bridges and steel structures generally are widely considered in public buildings, such as gymnasium, train stations and conference centres. The failure of these structures may cause huge loss of properties and even human's lives. In addition, these structures are often temporary shelters for people after severe earthquakes. Therefore, this kind of structures is often of high safety level and should be designed carefully to prevent the structures from collapsing even under the action of the severe earthquake.

There are several methods for seismic structural design, response spectrum method (RSM) is the conventional approach for seismic design of building structures. RSM accesses the maximum response of multi-degrees-of-freedom systems under earthquake load based on mode superposition method and response spectrum theory of single-degree-of-freedom (SDF) systems. Thus, RSM is applicable only to dynamic analysis of building structures with linear elastic behaviour.

Nonlinear time history analysis (NTHA) is the most commonly used approach to determine the elasto-plastic dynamic response of building structures under severe earthquakes. NTHA solves the dynamic response of building structures by direct numerical integration of dynamic equilibrium equations. The result of NTHA is accurate for specific ground motions. However, NTHA is time-consuming, dependent of the selection of ground motions and sometimes too complicated for common structural engineers, which hamper its application in engineering practice.

With the development of performance-based seismic design concept, pushover analysis (PA) began to be another effective tool for seismic design of structures. In pushover analysis, a structure is pushed with certain distributed loads until a predetermined target displacement is reached, to estimate the seismic behavior of the structure under severe earthquakes.

1.2 Research Problem

Many researchers conducted several studies on the steel trusses studying several aspects of structural design, but few studies focused on the seismic vulnerability of the steel truss bridges. Moreover, a parametric study is needed to investigate the maximum displacement in case of both simply supported and continuous steel truss bridges.

No previous studies adopted the non linear static or dynamic method for seismic evaluation of steel trusses bridges as the main concern of the steel truss bridge is the gravity loads or the wind loads.

1.3 Research Objectives

- Design a double Warren truss which is selected to provide an adequate lateral bracing to the bridge on the top and bottom using the commercial software SAP2000, based on AASHTO specifications.
- Analyse the steel truss bridge for several models, calculate the target displacement and generate the pushover curve in order to analyse and find the plastic hinges and failure positions.
- Generate new models to study the ductility of the steel trusses, the trusses will be studied in this thesis are both continuous and simply supported, the span length parameter effect will be studied.
- Study the nodes displacement for both horizontal and vertical earthquakes. Moreover, the effect of steel yield stress parameter on the maximum displacement values will be studied using one of the proposed models.

1.4 Research Methodology

Finite element model will be setup for the steel truss structure with commercial finite element software SAP2000, structural design will be conducted. All steel truss joints will be assumed to be hinge joints and the members subject only axial forces, either tension or compression. The material model for the steel is idealized elastic-plastic material. If the axial stress of a member reaches the yield stress of the material, a plastic hinge is thought to be generated at that location, which means the complete yield of the axial loaded member.

Parametric Study will be done in order to find the ductility factor using first yield and ultimate yield values for the different steel truss structures. Continuous and long span truss bridges will be also evaluated and the level of performance will be checked after excessive loads. Parametric study will be conducted on series of 2D steel truss bridge models in order to study the maximum displacement values and the yield stress effect.

1.5 Research Outline

The thesis consisted of five chapters; each chapter contains the following parts:

Chapter 1: Introduction, research Problem, objectives and methodology

Chapter 2: Experimental Investigation in the Literature review

Chapter 3: FE Modelling Parameters and Seismic Design Modelling of Steel Structures

Chapter 4: Results and Discussion (pushover curve, ductility results and maximum displacement values)

Chapter 5: Some important Conclusions and Recommendations

Chapter 2: Literature Review

2.1 General Introduction

Railway and highway bridges are playing an important role in transportation systems in any modern country as important means of transportation. Bridges response under major seismic actions depends on their energy-dissipation capacity. Weak beam strong column building philosophy is adopted for energy dissipation. However, bridges designed to bear the damage and plastic hinges need to be formed in abutment and piers or only in piers for energy dissipation. Furthermore, it is necessary that under gravity loads, inelastic actions should be at available locations and should not cause any failure. For earthquake-resistant design, damage should not occur in brittle mode and should be in ductile mode so there will be warnings and the ultimate strain values will take time to reach so there will be enough time to rehabilitate and retrofit these structures. It is achieved using the capacity design method to avoid undesirable failure modes (Satish et al., 2022)

The focus of seismic design in current building and bridge codes is one of life safety without the ability to consider multiple levels of structural performance from various loading conditions. Consequently, although collapse is prevented for the design seismic loading, there is no guarantee that the structure will remain usable and may therefore have to be demolished upon occurrence of an earthquake with an intensity comparable with the design intensity. Although the loss of life is prevented, the economic losses can be staggering. There is also no procedure for designing against earthquakes greater than the prescribed return period of 475 years. For a seismic event of greater magnitude, all structures are subject to collapse. (Floren and Mohammadi, 2001) conducted a critical evaluation of these performance criteria and their relevance to highway bridge design, in conjunction with the current design practice, is discussed. Various types of designs such as those based on strength, deformation, nonlinear behavior, and energy, which can be used to meet the specified performance levels in seismic design of highway bridges, are also discussed. Performance of the bridges is based on the structure, structure deformation level, soil type, and structural member's ductility, mainly supports and piers. (Machida and Khairy Hassan, 2000) stated that failure modes change the severity of the diagonal failure of bridges. For this, the authors proposed the direct displacement-based assessment method to calculate the safety factor compared with Incremental Dynamic Analysis.

2.2 Seismicity in Israel

The main seismic sources are faults and fault zones that are likely to generate significant (> 6) earthquakes in Israel. The only two instrumentally recorded significant earthquakes are the 1995 7.2 MW Nuweiba earthquake occurred on the Aragonese Fault which was associated with mean slip of 1.4–3 m (Baer et al., 1999) and the 1927 6.25 ML Dead Sea earthquake, which result in hundreds casualties and a severe damage. All other information is based on geodetic, geologic, prehistoric and historic evidences (Klinger et al., 2015; Sadeh et al., 2012; Zohar et al., 2016). The faults constitute potential sources for earthquakes that can cause different sorts of damages, including ground motion and acceleration, landslides, liquefactions, surface rupture and tsunamis. The map is essential for seism tectonic modeling of Israel, probabilistic seismic hazard analysis (PSHA) and eventually for generating ground motion maps.

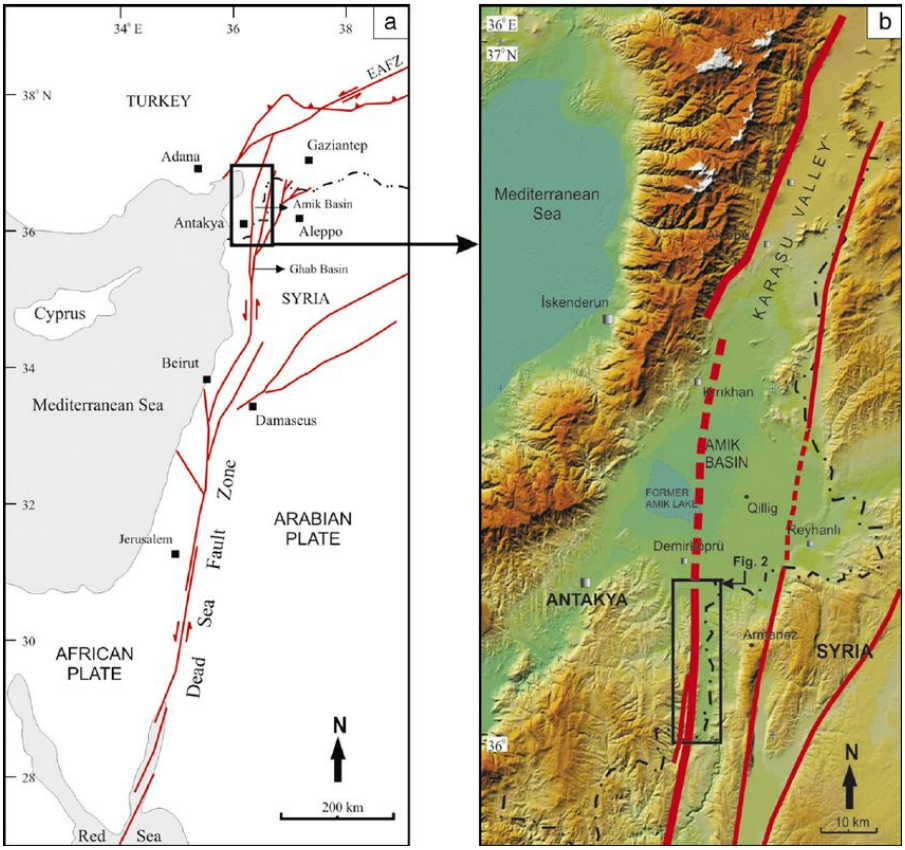

Figure 1 General Map of Dead Sea Fault Zone

The mapped faults are also important for establishments of standards, such as Israeli standard SI 1227 for bridges. The traces of most of the faults in the map are located and mapped using 1:50,000 geological maps of Israel of the geological survey of Israel. Fault beyond the Israeli borders, inferred subsurface fault continuations, and inferred submarine faults are mapped based on the references listed in table 1. The certainty in the locations and even in the existence of some of the inferred faults can be low and should be better constrained in the future. Large earthquakes along the Cyprian Arc can generate tsunamis that might affect the coastline of Israel (Salamon et al., 2007).

Table 1 Faults beyond the Israeli borders and inferred faults

Geographic Location	Type of fault	Reference
Gulf of Eilat	Submarine Inferred Fault	(Ben-Avraham, 1985; Hartman et al., 2014)
Arava Valley	Beyond Israeli Borders	(Calvo, 2002; Le Béon et al., 2012; Sneh and Weinberger, 2014)
Dead Sea Basin	Subsurface inferred continuations of the main faults, Beyond Israeli Borders and Submarine Inferred Fault	(Ben-Avraham and Schubert, 2006; Sneh and Weinberger, 2014)
Jordan Valley	Beyond Israeli Borders	(Ferry et al., 2011; Sneh and Weinberger, 2014)
Gilboa Fault – Western Part	Subsurface inferred continuations of the main faults	(Sneh and Weinberger, 2014)
Carmel Fault – Eastern Part	Subsurface inferred continuations of the main faults	(Sneh and Weinberger, 2014)

Carmel Fault – Western Part	Submarine Inferred Fault	(Schattner and Ben-Avraham, 2007)
Haula Basin	Subsurface inferred continuations of the main faults and beyond borders	(Schattner and Weinberger, 2008)
Lebanon and Syria	Beyond Israeli Borders	(Garfunkel, 2014; Sneh and Weinberger, 2014; Weinberger et al., 2009)

Seismic hazard maps show the distribution of earthquake shaking levels that have a certain probability of exceedance. These maps were prepared in order to provide for the basic seismic requirements for the construction of safe buildings and bridges to withstand ground shaking from strong earthquakes. In 2001, the Israel Geological Survey defined the regional seism genic zones and these were approved in 2007, with minor changes, by experts from all neighboring countries. All together 27 seism genic zones were defined. The seismic parameters associated with each of the seism genic zones were defined by the Geophysical Institute of Israel. Those efforts have led to updating of the requirements in the Israeli Code 413 in terms of Peak Ground Acceleration, (PGA), for a probability of exceedance of 10% in 50 years (or return period of 475 years) for sites of generic rock with Vs=620 m/s. In the process of updating SI 413, the new seismic requirements are based on earthquake response spectral acceleration at two specific periods – short (T = 0.2 sec) and long (T = 1 sec) - that have a probability of 10% of being exceeded in an exposure time of 50 years (475 years return period) and damping ratio of 5%. The assessment of the new hazard parameters is also based on using the empirical ground motion attenuation equations developed by (Boore et al., 1997). (Zaslavsky et al., 2009) used commercial program EZFRISK is used for computing peak ground acceleration and Spectral Acceleration (SA) under the assumption that earthquake occurrence and it showed that the seismicity of the region is relatively low and can be explained by very long return period (hundreds and thousands of years) of strong earthquakes.

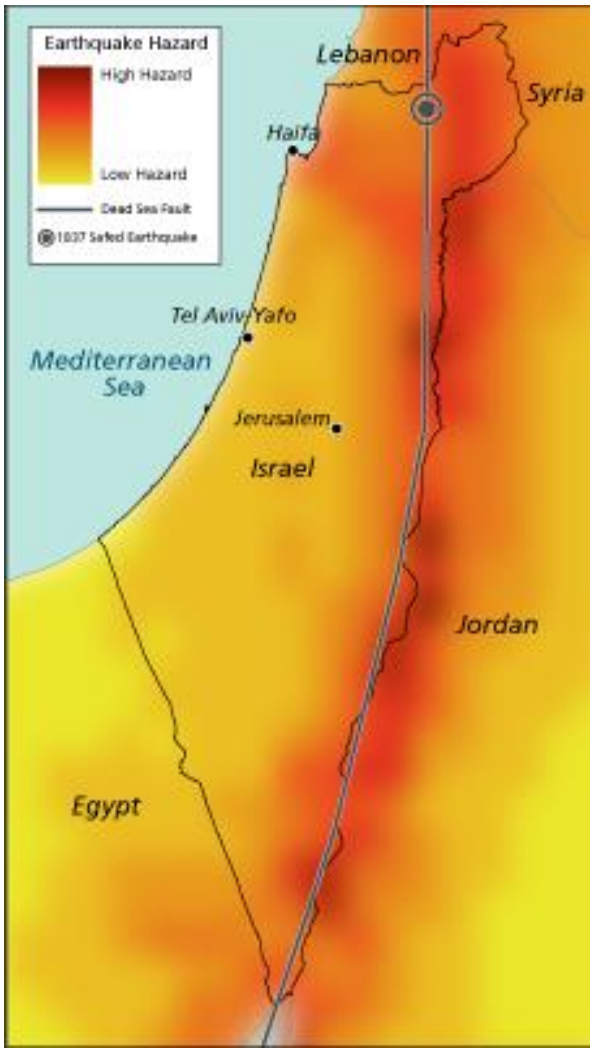

Figure 2 Seismic hazard map of Israel

Israel lies between the African and Arabian plates, whose movement away from each other is a major source of seismic activity from the Azores in the Atlantic Ocean all the way to the Hindu Kush in Afghanistan. The Arabian plate is moving north, away from the African plate, along the Dead Sea transform fault, which serves as a boundary between the plates (Figure 3). Israel sits alongside this left-lateral strike-slip fault that extends 1,000 km (600 miles) from the Red Sea Rift and the Gulf of Aqaba in the south, across Israel, Jordan, Lebanon, and Syria, to southeastern Turkey.

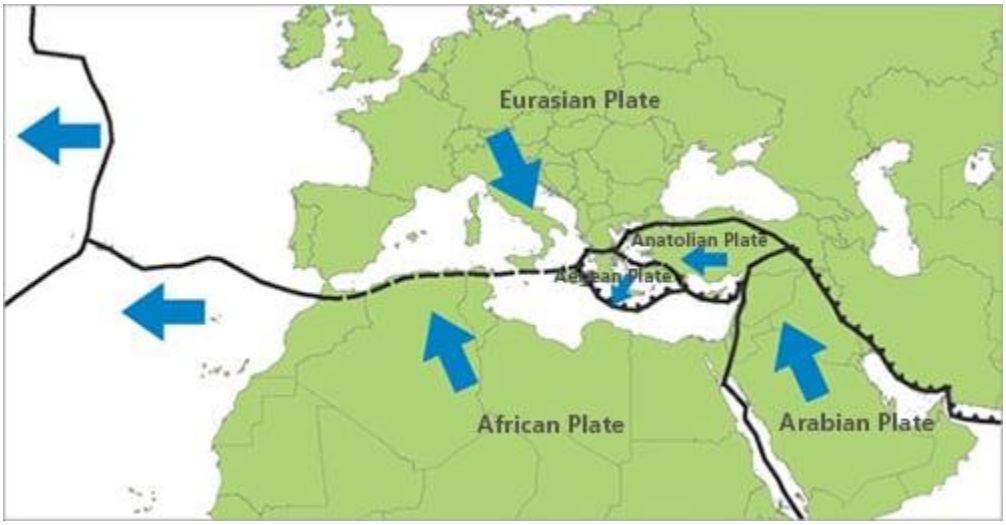

Figure 3 Tectonic setting of the Pan-European region

The epicenters of most earthquakes in Israel—including the Safed earthquake—are located either in or near the Jordan Rift Valley, through which the fault extends. The epicenter of the M7.1 1837 quake is believed to have occurred on a segment known as the Roum fault in the Jordan Rift Valley. The quake killed more than 5,000 people and caused massive damage in the cities of Safed and Tiberias. The city of Safed was almost destroyed, and almost every home in the nearby town of Jish was demolished. In addition, many towns and villages in the epicentral region were built on hilltops or steep slopes, and landslides were reported throughout the area. If the Safed earthquake were to recur today, it would exceed EUR 3.3 billion based on the present-day building stock.

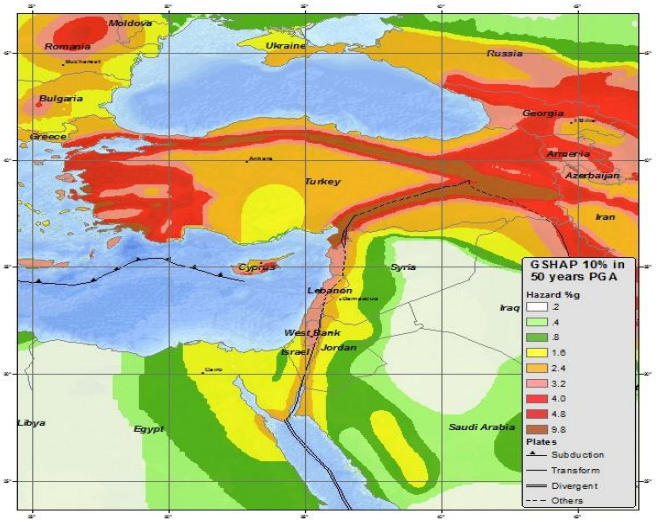

Figure 4 Hazard based on historic earthquakes

Many seismologists have said that “the earthquakes don't kill people, their structures do”, this is because most deaths from earthquakes are caused by main damage of structures or other human construction falling down during an earthquake. So, before any assessments start, a good practice to study two fundamentally different concept of the hazards and risk. In general terms, Risk, in its simple manner, is the probability of harm if someone or something that is vulnerable to expose the hazard, the hazard can be defined as a phenomenon that has potential to cause harm. Phenomena are both natural and man-made. For example, earthquakes, hurricanes, fires, and floods are natural hazards; whereas car crashes, and terror attacks are man-made hazards.

$$\text{Seismic risk} = (\text{Seismic hazard}) \times (\text{Vulnerability}) \times (\text{Value})$$

Where Vulnerability is the amount of damage induced by a given degree of hazard, and expressed as a fraction of the Value of the damaged item under consideration.

2.3 Response of Steel Bridges under Seismic Actions

Types of bridges consists of mainly of prestressed concrete, reinforced concrete and steel superstructures. The steel bridge consists mostly of simply supported and continuous steel girder bridges resting on expansion bearings and fixed bearing. In this section, the literature available for the performance and behavior of steel bridges will be reviewed. Typical damage seen in previous events includes damage to non-ductile columns, failure of fixed bearings, instability and overturning of rocker-type expansion bearings, and damage to the abutments (Choi and Jeon, 2003).

The behavior of steel girder bridges, both continuous and simply supported, under low-to moderate shaking has been studied to understand what details pose the greatest risk for damage. (Itani et al., 2004) studied the seismic behavior of steel girder bridge superstructures. Bridge superstructures, both with cross-frames and without, were modeled in SAP90 to determine the effect of cross frames on the performance of the bridge under seismic loading. For bridge superstructures without cross frames, the bridge deck was found to behave as a rigid body and displace linearly and the flexible steel girders were found to twist and deform laterally as needed with the most distortion near the supports as the bearings are the only points which counteract that movement. For bridges with

intermediate cross frames, but no end cross frames, the behavior was found to not improve much as most of the distortion occurs near the supports. Analysis of bridges with intermediate and end cross frames showed that a minimal stiffness of the end cross frames was sufficient to allow the superstructure to behave as a unit.

The seismic fragility of typical steel bridges in moderate seismic zones was studied by (Choi and Jeon, 2003), the response of typical bridges was studied with and without retrofit measures. The retrofit measures investigated included replacing steel bearings with elastomeric bearing, adding restrainer cables at supports, and using a combination of both elastomeric bearing pads and restrainer cables. The major findings were that the superstructures remain linear, but the substructure units do not. Therefore, it is important to define the moment-curvature relationship of the substructure to understand the nonlinear behavior. It was found that using elastomeric bearing pads instead of steel bearings had a good isolation effect, but the bearing pads cannot protect the damage from pounding of the superstructure and abutments effectively.

(DesRoches et al., 2004) conducted an experiment to understand the effects of the 475-year earthquake and the 2.475-year earthquake on the response of multispan simply supported (MSSS) and multispan continuous (MSC) steel girder bridges in the central and southeastern United States (CSUS). 95% of bridges in CSUS were found to be are MSSS bridges, MSC bridges, or single span bridges and one third of these bridges are steel girder bridges. A bridge model, using typical details and properties found in CSUS, was developed for both a MSSS bridge and a MSC bridge using DRAIN-2DX. Each girder was supported by a fixed bearing or an expansion bearing. The bridge substructure was modelled using multi-column bents and pile bent abutments. The deck was modelled using linear elements since it is expected to remain linear. The columns were modeled as fiber elements with a defined stress-strain relationship to account for the distribution of inelastic deformation. The steel bearings were modelled using the analytical model previously developed by (Mander et al., 1996).

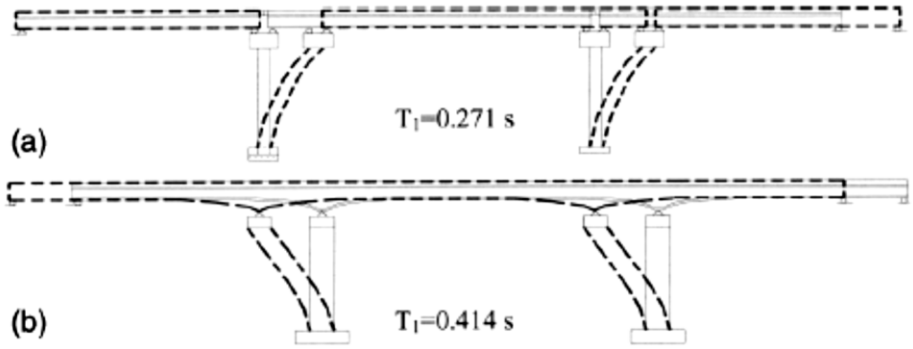

Figure 5 Mode Shapes for (a) Multispan Simply Supported Steel Girder Bridge and (b) Multispan Continuous Steel Girder Bridge (DesRoches et al., 2004)

Ground motions typical for CSUS were applied to the model to determine the behavior of these bridges. The MSSS bridge had a fundamental period of 0.27s where the fundamental mode was the two frames moving linearly with one frame remaining stationary. The MSC bridge had a fundamental period of 0.41s where the fundamental mode was the longitudinal translation of the continuous deck (DesRoches et al., 2004). The fundamental modes can be seen in Figure 5. The findings from this study reinforced the understanding of typical deficiencies seen after large event. The column demand on the MSC was two times larger than that on the MSSS due to a larger mass and displacement associated with the MSC bridges. The impact between decks of MSSS bridges and between the deck and the abutment of MSC bridges will likely lead to failure of the steel bearings. Deck displacement often exceeded the limit on rocker bearings and lead to toppling of the rocker bearing.

A deeper look into the seismic fragility of continuous steel highway bridges in New York was conducted by (Pan et al., 2007). Using SAP2000, a three-dimensional model of a typical bridge was developed. In the transverse direction, displacement was restrained by both fixed and expansion bearings and inertial forces are transferred. The longitudinal direction is the critical direction and the columns were modelled as vertical cantilevers with a single plastic hinge forming at the base of each column. The moment-curvature relationship was defined to understand the nonlinear effects. Both fixed and expansion bearings were included in the model with the fixed bearing on one intermediate pier,

allowing rotation only, and the expansion bearings at the abutments and the other intermediate piers, allowing both rotation and translation. The expansion joints were modelled as gap elements to understand the effects of pounding on the behavior of the bridge A major finding from this study was that the gap size has a significant effect on column ductility during large ground motions. Additionally, the bridge response is more sensitive to reinforcement yield strength than column concrete compressive strength. The friction coefficient of the expansion bearing has a significant impact on the behavior. Ignoring the friction is an over-simplification of the expected bearing behavior whereas overestimating the friction factor can lead to larger forces transferred to the column.

Typical abutment types include integral, semi-integral, and non-integral abutments. Non-integral abutments are identified by the presence of an expansion joint. The most common problems with non-integral abutments is unseating of the superstructure from the bearing and pounding of the approach spans. This problem is eliminated for semi-integral and integral abutment bridges since the expansion joint is eliminated. The connection between the superstructure and the abutment for integral and semi-integral abutments allow the bridge to move together as a monolithic structure. (Frosch et al., 2009) studied the seismic behavior of typical integral abutment details, laboratory testing of the current integral abutment details was used to determine the displacement capacity of the current design and analytical models were used to estimate the seismic displacement at the abutments. The findings were that for bridges up to 500 ft, the current design for the integral abutments was adequate to provide seismic resistance, and for bridges greater than 500 ft in length, additional confinement at the pile head was needed for adequate seismic resistance.

The New York State Department of Transportation (NYSDOT) developed a Seismic Vulnerability Manual in 1995 which describes a detailed methodology for evaluating the highway structures for seismic vulnerability. The methodology flowchart, shown in Figure 6, consists of a screening process, a classifying process and a rating process. The screening process consists of a preliminary screening, in which bridges that do not need an assessment and bridges that need a more detailed assessment are identified, and a secondary screening, in which the bridges to be assessed are assigned a susceptibility group based on their details. The preliminary screening removes tunnels and culverts, bridges that

are currently closed, and bridges with complex structural elements, such as arch and stayed girder bridges. The secondary screening classifies bridges into one of four susceptibility groups: high seismic vulnerability, high-moderate seismic vulnerability, moderate-low seismic vulnerability, and low seismic vulnerability. Bridges identified as high seismic vulnerability consist of multispan simply supported bridges with rocker bearings, a skew greater than 30 degrees, or with fewer than four girders. Bridges identified as moderate-high seismic vulnerability consist of all the other multispan simply supported bridges, multispan continuous bridges with rocker bearings, a skew greater than 30 degrees, or with fewer than four girders, single span bridges with rocker bearings, a skew greater than 30 degrees, or with fewer than four girders, and bridges with unreinforced piers. Bridges identified as moderate-low seismic vulnerability consist of bridges with steel pile piers and bridges with a single column pier. The bridges identified as low seismic vulnerability are those with integral abutments. The classifying process produces a score for each bridge which quantifies potential vulnerability relative to other bridges and places bridges into high, moderate, and low seismic vulnerability classes. The score is based on a vulnerability score and a seismic hazard level. The vulnerability score is calculated using various bridge details such as the substructure dimensions, the reinforcement ratio of the substructure, the bearing type, and the seat width at expansion joints. The seismic hazard level is based on an effective peak acceleration at a site with a return period of 475 years and requires the soil type at each site. The rating process provides a uniform measure of a structure's vulnerability to failure based on a likelihood score and a consequence score. The likelihood score is based solely on the classification level whereas the consequence score is based on a failure type score and an exposure score. NYSDOT uses the ratings to determine the action required to reduce the failure vulnerability of the bridge. These actions include, but are not limited to, a safety program watch, a safety program alert, a capital program, and an inspection program (NYSDOT, 2004) The Federal Highway Association (FHWA) created a seismic retrofitting manual for highway structures very similar to the one used by NYSDOT. This manual describes the seismic hazard, presents methodologies for screening, prioritizing, classifying, and evaluating structures, and 30 describes different retrofit options for different details found to be vulnerable. The screening, prioritizing and classifying methods result in a uniform measure of a structures seismic vulnerability to an

upper level earthquake ground motion (that with a return period of approximately 1000 years) and a lower level earthquake ground motion (that with a return period of approximately 100 years) (Buckle, 2006). The methodology used to develop NYSDOT's Seismic Vulnerability Manual and FHWA's Seismic Retrofitting Manual has be used in many research applications. In Kentucky, the bridges along I-24 have been evaluated and ranked using the FHWA methodology. The results from this study prioritized the bridges for a detailed evaluation (Zatar et al., 2006).

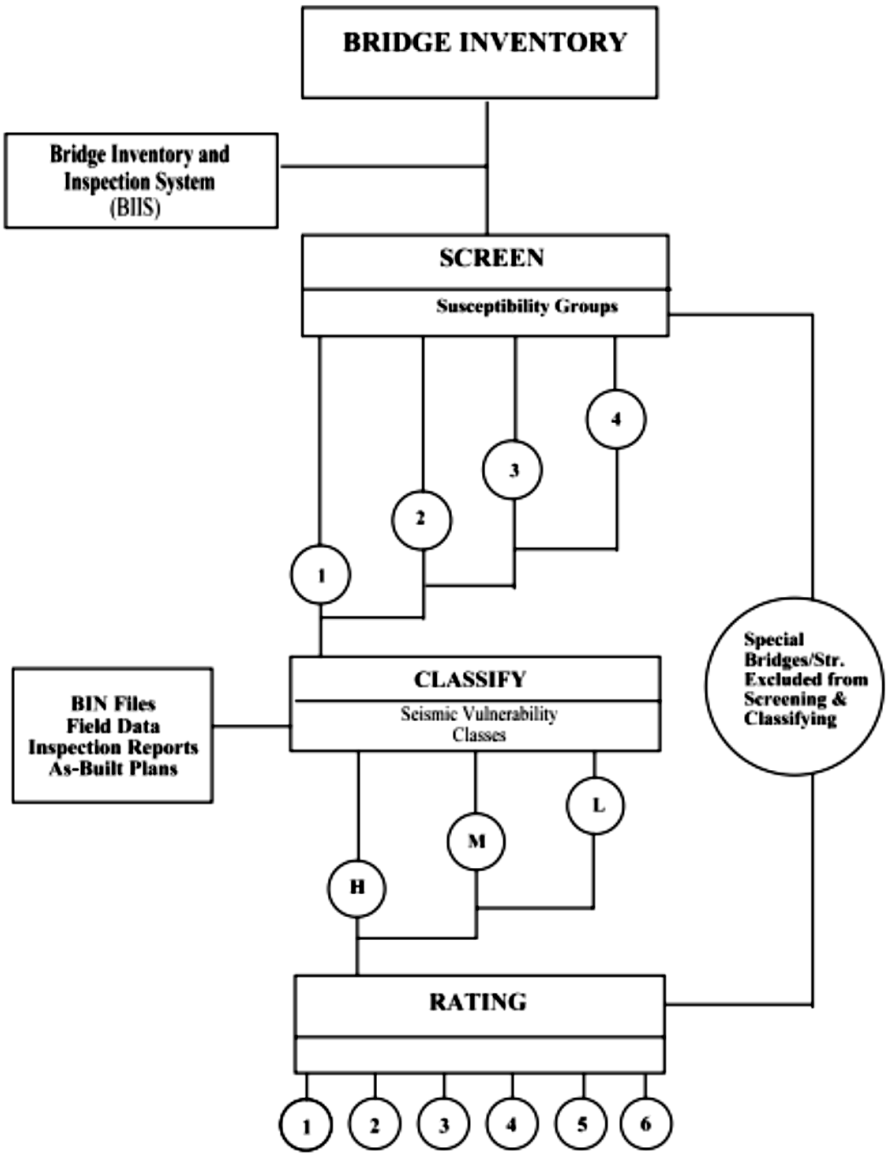

Figure 6 seismic vulnerability flowchart (NYSDOT (2004). Seismic Vulnerability Manual. New York State Department of Transportation, New York, NY.)

The National Bridge Inventory Data Federal Highways Administration (FHWA) revealed that 58.2% of the highway bridges in New York State are multibeam slab-girder types. According to the distribution of classification on material type, 65.6% of the bridges have steel superstructures. Traditionally, only multispan bridges are studied for seismic risk while no detailed seismic analysis is usually required for single span bridges. In general, multiple span bridges can be either simply supported i.e., multispan simply supported MSSS bridges or continuous with various superstructure types, such as steel girder, prestressed concrete multiple box beam, prestressed concrete girder. In New York State, 70% of the multispan bridges are simply supported steel bridges and 27% are multispan continuous steel bridges. MSSS steel bridges typically have two or three spans with maximum span lengths in the range of 10–20 m. (Pan et al., 2010a) presented the results of the nonlinear dynamic seismic analysis of MSSS bridges in New York State, including the development of a three-dimensional finite-element model, the execution of a parametric analysis, the review of bridge uncertainties and model sampling, the estimation of seismic capacity, the simulation of ground motions, and the design of two common seismic retrofit measures. This research showed the seismic fragility analysis of typical MSSS bridges without and with retrofits, which was presented in (Pan et al., 2010b).

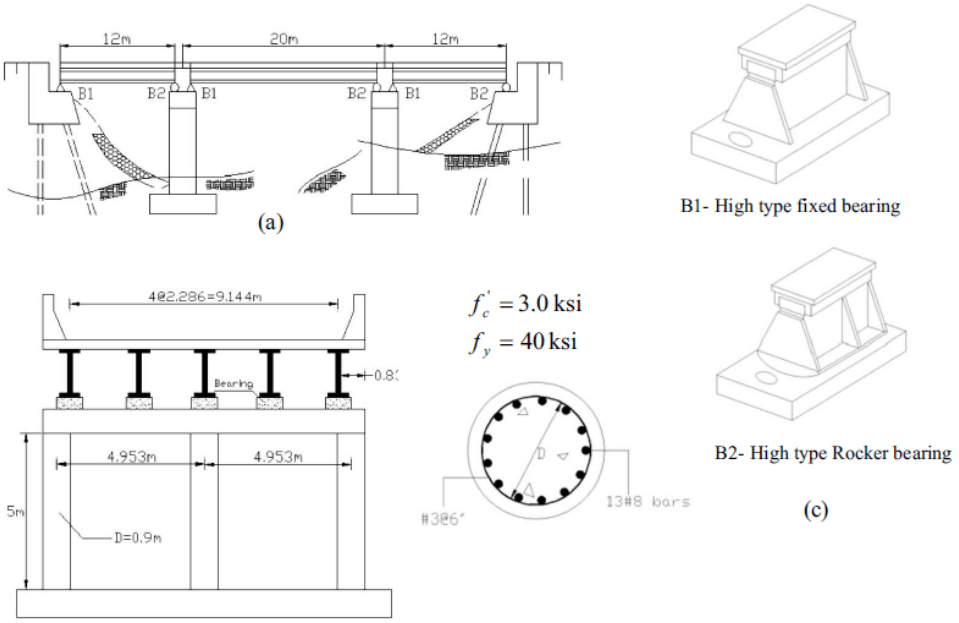

Figure 7 Configuration of a typical MSSS steel girder bridge (Pan et al., 2010b)

2.4 Seismic design approaches of structures

Response spectrum method (RSM) is the conventional approach for seismic design of building structures. RSM accesses the maximum response of multi-degrees-of-freedom systems under earthquake load based on mode superposition method and response spectrum theory of single-degree-of-freedom (SDF) systems. Thus, RSM is applicable only to dynamic analysis of building structures with linear elastic behaviour.

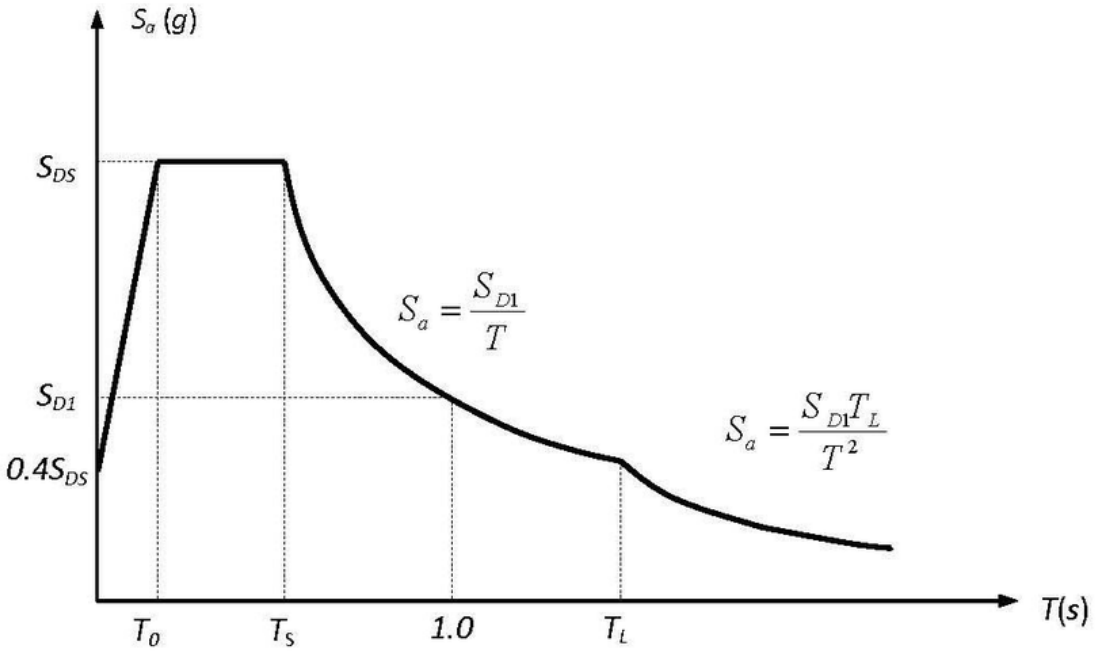

Figure 8 Design Response Spectrum

Nonlinear time history analysis (NTHA) is the most commonly used approach to determine the elasto-plastic dynamic response of building structures under severe earthquakes. NTHA solves the dynamic response of building structures by direct numerical integration of dynamic equilibrium equations. The result of NTHA is accurate for specific ground motions. However, NTHA is time-consuming, dependent of the selection of ground motions and sometimes too complicated for common structural engineers, which hamper its application in engineering practice.

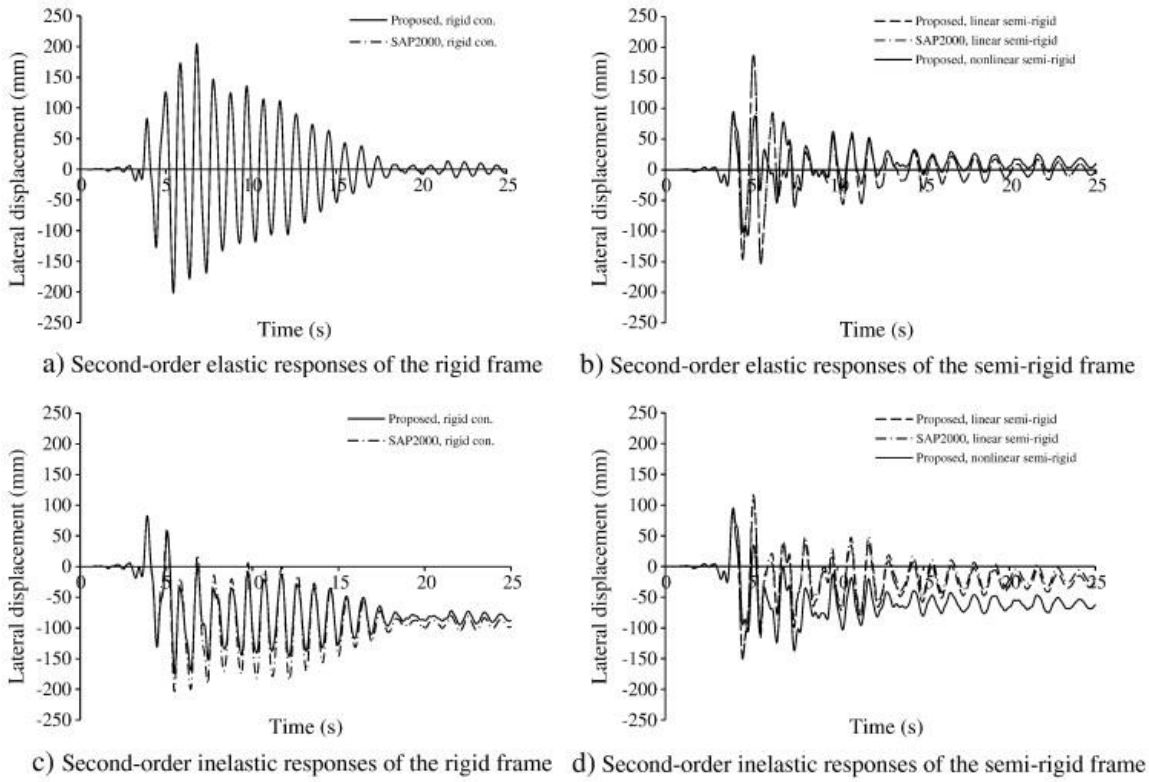

Figure 9 Lateral displacements from NTHA (Nguyen and Kim, 2014)

2.4.1 Pushover Analysis

With the development of performance-based seismic design concept, pushover analysis (PA) began to be another effective tool for seismic design of structures.(Comartin, 1996; Walls, 2004). In pushover analysis, a structure is pushed with certain distributed loads until a predetermined target displacement is reached, to estimate the seismic behavior of the structure under severe earthquakes. Lots of research works have been done on pushover analysis of high-rise buildings (D'Ambrisi et al., 2009; Di Sarno and Wyatt, 2006; Yin et al., 2019) and the accuracy of pushover analysis has been verified by comparing with the results of NTHA (Causevic and Mitrovic, 2011; Huang and Kuang, 2010; Kim and D'Amore, 1999; Moghaddam and Hajirasouliha, 2006) and shaking table tests (Cardone, 2007).

Capacity curve is a characteristic curve to be defined by a pushover analysis, where the displacements are plotted versus the base shear, the target displacement can be calculated using the intersection of the capacity spectrum and the demand spectrum which is determined by iteration calculation of capacity spectrum method CSM as shown in figure

10. However, pushover analysis can also estimate the strength capacity of a structure beyond its elastic limit up to its ultimate strength in the post elastic range. In the process, the method also predicts potential weak areas in the structure, by keeping track of the sequence of damages of each and every member in the structure by use of what are called hinges.

Different ways for the application of the load can be performed, for defining different types of pushover analysis. A monotonic pushover analysis considers a monotonic lateral load pattern which pushes the structure until the lateral capacity is reached; therefore the capacity of the structure is dependent mainly on the loading pattern.

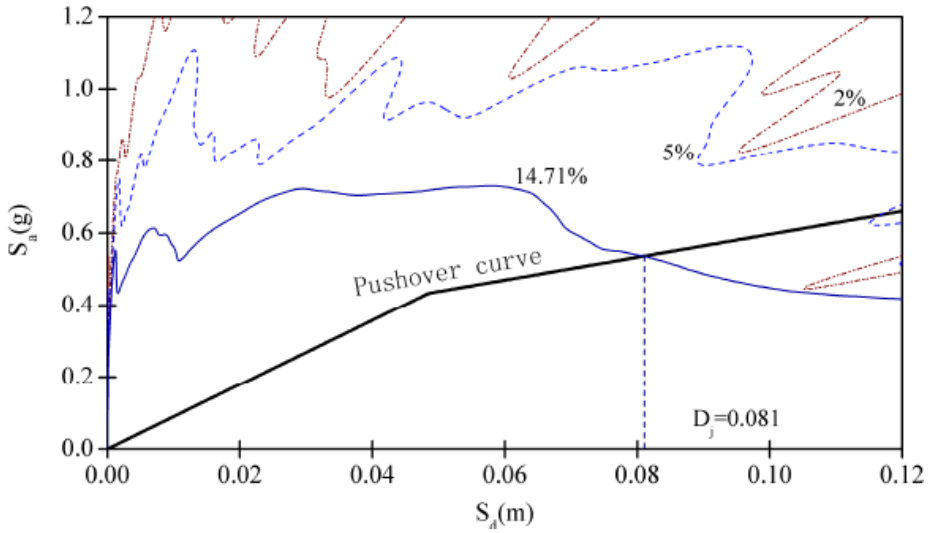

Figure 10 Target displacement using CSM (Yin et al., 2019)

(Yin et al., 2019) conducted a study on long span steel structure using the pushover analysis and it was found by the study that the seismic behavior of this kind of long-span steel truss structures can be evaluated by traditional pushover analysis accurately enough for practical design purpose. Pushover analysis has been adopted in the seismic analysis of long-span steel structures by other researchers and engineers (Fu et al., 2005; Pan and Ohsaki, 2006; Paraskeva et al., 2006; ZHANG and QIAN, 2010) However, pushover analysis is based on the assumption that the dynamic response of the structure is controlled by the elastic fundamental mode, which is the case for most regular high-rise buildings (Elnashai and Di Sarno, 2015). Due to their large number of degrees of freedom, long-span steel structures

often have densely distributed natural frequencies and complex vibration modes. The accuracy of pushover analysis is then often questioned because the above assumption may not be satisfied. Though some modified pushover procedures (Chopra et al., 2004; Chopra and Goel, 2002) have been presented to consider the effect of high-order vibration modes, they all improve the accuracy of pushover analysis at the expense of losing the simplicity of traditional pushover analysis. In addition, different from high-rise buildings, vertical earthquake should also be considered in the seismic design of long-span steel structures. Therefore, it is desired that the accuracy of traditional pushover analysis can be evaluated for long-span steel structures.

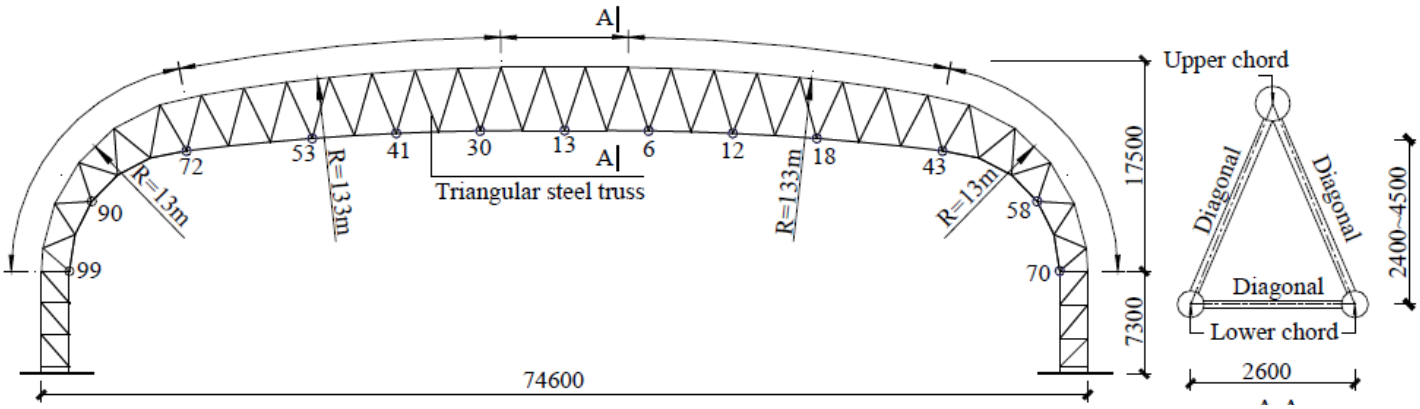

Figure 11 Configuration of the long-span steel truss structure studied by (Yin et al., 2019)

2.5 Relevant Codes and Standards

The codes and standards which are studied to resist progressive collapse of the steel bridge, and to determine deficiencies that may exist in the analysis for existing steel truss bridges. The current codes and standards will be summarized starting from American standards to European codes, in order to find differences that may exist.

2.5.1 IBC 2012

The International building code (IBC) 2012, establish the foundation for minimum requirements considering buildings and public safety. In particular, for high rise buildings, or high risk regions, IBC, lays out, the requirements to ensure the structural integrity, also for load bearing structures, the vertical ties are required in all walls, in addition to transversal, longitudinal ties at each floor. IBC goes on, to provide design methods and equations in order to meet these design requirements.

2.5.2 ASCE 7-10

The American Society of Civil Engineers (ASCE) 2010, in similar manner, provides minimum design requirements for buildings through the United States. ASCE provides a minimum requirement for structural integrity for all buildings, in particular, the section 1.4 of ASCE 7-10 states that "all structures must have a continuous load path for the structure and a lateral force resisting system capable of resisting the appropriate notional loads for each level derived from the structure's weight".

The commentary of section 1.4 indicates that these requirements are intended for "normal service and minor unanticipated events".

ASCE 7-10 also, provides load combinations for design, in two general approaches, known as direct and indirect, and provides guidelines for the provision of general structural integrity, as shown below: Indirect Design: defined in ASCE 7-10 as "implicit consideration of resistance to progressive collapse, during the design process through the provision of minimum levels of strength, continuity, and ductility". The indirect design method will be difficult to use for existing masonry buildings, due to the addition of ties. Direct Design: defined in ASCE 7-10 as "explicit consideration of the resistance to progressive collapse during the design process". Two procedures, known as alternate path method and specific local resistance method, are presented to accomplish this consideration. These procedures allows local failure to occur, but seeks to provide alternate load paths so that the damage is absorbed and major collapse is averted" while the local resistance method "seeks to provide sufficient strength to resist failure from accidents or misuse".

2.5.4 GSA 2013

The General Service Administration (Alternate Path Analysis and Design Guidelines for Progressive Collapse Resistance) which is known shortly as General Services Administration, (GSA, 2013), publish the latest previsions in October 2013 and replaced the document "GSA Progressive Collapse Analysis and Design Guidelines for New Federal Office Buildings and Major Modernization Projects" which was published in June 2003. The new provisions have good modifications which can be summarized as elimination of the tie force method and the local resistance method, which presented in Unified Facilities Criteria (UFC) 04-023-03: Design of Buildings to Resist Progressive Collapse for all materials, which leave only the alternative path method for design and analysis.

2.5.5 UFC 04-023-03

Design of Buildings to Resist Progressive Collapse, (Department of Defense, 2009), shows the guidelines for progressive collapse were updated in 2009. These guidelines are written by the United States Department of Defense, and state three different design procedures that can be used with masonry, such that, tie force, alternate path , and Enhanced Local Resistance. Occupancy category ensures for applying the tie force and enhanced local resistance procedures, but when tie force requirements cannot be met, the alternate path method must be used. It is noted within the UFC that the alternate path method is "often the most practical choice" for load bearing wall structures.

2.5.6 ASCE 41-13

American Society of Civil Engineers, 2014, (ASCE 41-13) is referenced by UFC 04-023-03 for analysis procedures with respect to the building material of the structure. All details and material sections in ASCE 41-13 provide analysis guidelines such as modeling criteria, acceptance criteria, and strength calculations. For the strength calculations as an example, it lacks in some areas when compared to the steel and concrete sections of the standard. These areas include information about recommendations for retrofit strategies.

2.5.7 EUROCODE

This national standard for European countries lays out guidelines and requirements for designing buildings to resist progressive collapse. Euro code: Basis of Structural Design (EN 1990) sets out the general requirements for structural design by stating "A structure shall be designed and executed in such a way that it will not be aged by events such as: (1) explosion, (2) impact, and (3) the consequences of human errors, to an extent disproportionate to the original cause" (European Committee for Standardization, 2001). It continues on to state that this shall be avoided or limited by selecting and designing a structural system such that it can survive adequately from the accidental removal of an individual member (aka: progressive collapse) Euro code 1 – "Actions on structures – Part 1-7 (EN 1991-1-7): General Actions – Accidental Actions" (European Committee for Standardization, 2006): This section gives more specific requirements for progressive collapse actions on structures and the strategies that should be used to prevent progressive collapse depending on the risk category of the structure.

Chapter 3: Seismic Design Modelling of Steel Structures

3.1 Design of steel structures standards

The evolution of the seismic design of steel structures in the past half-century can be roughly divided into three eras. Prior to 1988, both general seismic loading provisions and material-related seismic design provisions (including those for steel structures) were typically integrated in a single document: the locally adopted model building code. In those days, seismic design of low-rise and midrise buildings without major irregularities used the "equivalent lateral force" method. For example, in the 1985 Uniform Building Code (UBC) (ICBO 1985) the base shear for working stress design was specified as

$$V_w = (ZIKCS)W$$

where the horizontal force factor, K = factor accounting for the relative ductility and energy dissipation of building systems. Buildings were grouped into four types based on their earthquake-resisting elements, with K equal to 0.67, 0.80, 1.0, and 1.33 for seismic force–resisting systems (SFRSs), respectively, defined as moment-resisting frame systems, dual systems, building frame systems (for all systems not in the other three categories), and bearing wall systems. For steel buildings, only the ductile moment resisting space frame (DMRSF) could be designed for the lowest seismic base shear, with K ¼ 0.67. For application in high seismic regions, additional design requirements were few. The only requirement for members of steel DMRSFs was that "Members in which hinges will form during inelastic displacement of the frames shall comply with the requirement for plastic design sections." For capacity design, it was specified that "Each beam or girder moment connection to a column shall be capable of developing in the beam the full plastic capacity of the beam or girder." For braced frames in moderate to high seismic regions, all members needed to be designed for 1.25 times the prescribed seismic forces; connections needed to be designed to develop either the full capacity of the members or the prescribed seismic forces without the one-third increase usually permitted in working stress design for stresses resulting from earthquake forces. Significantly, these requirements were based on the SEAOC recommendations (SEAOC 1980).

The 1988 edition of the UBC (ICBO 1988) began the second era of seismic steel design. On the seismic loadings side for base shear calculation, this edition abandoned the format of previous Eq., that relied on empirical K factors. Instead, a response modification factor, Rw, was used to calculate Vw for working stress design, where :

$$V_w = (ZIC/R_w)W$$

Based on the vertical components in the SFRS, each category was further divided into several classes with their associated Rw values. More significantly, specific ductility design requirements for special moment-resisting space frames (SMRSFs), concentrically braced frames (CBFs), and eccentrically braced frames (EBFs) were provided; a prescriptive girder-to-column moment connection for SMRSFs was codified; and the concept of capacity design was introduced (e.g., prescribing the use of amplified seismic load to protect columns from global failure). Based on the 1988 UBC, the first edition of the AISC Seismic Provisions was published in 1990 (AISC 1990). This seismic steel design practice continued through the 1994 UBC edition. The trigger for the third era, as far as seismic steel design is concerned, was the Northridge, California, earthquake that occurred on January 17, 1994. This event drastically changed the seismic research, design, and construction of steel buildings in the United States and is fully addressed in a subsequent section. For most of the previous century, three model building codes were predominantly and broadly used in different parts of the United States (a model building code serves as a reference, being adopted with or without modifications by local building codes in the United States, which has no mandatory national code). In the 1990s, there was an effort to unify all three codes into one, resulting in the creation of the International Building Code (IBC), which references ASCE 7 (ASCE 2016) for its design earthquake loads and the AISC Seismic Provisions for its seismic steel design requirements. To provide specific design requirements for the SFRSs listed in ASCE 7, starting with the 2010 edition, the AISC Seismic Provisions grouped steel SFRSs into the two categories: moment frame systems as well as braced frame and shear wall systems. Although it appears that the ASCE 7 standard covers the required seismic forces (i.e., the load effect side) and that the AISC Seismic Provisions deal with design strengths (i.e., the resistance side) of steel members and components, these two standards are related to each other in an implicit, yet significant,

way through the response modification factor, R. Furthermore, because the seismic load effect is also coupled with the actual strengths of the members and the entire structure, the AISC Seismic Provisions cover requirements not only for the resistance side but also for the required earthquake load effect side. Ductility design and capacity design are two pillars of the seismic design of structures. To pave the way for the presentation to follow, the relationship between these two design concepts and the R factor approach is briefly presented next.

3.2 Ductility Design, Capacity Design, and R Factor

The expected structural response of an SFRS designed for a design earthquake are shown in the following figure 12. Point E represents the required seismic force level if the structure remains elastic. Because this force level can be high, say above 1 g times the reactive seismic mass of the building in high seismic regions, modern seismic codes accept the concept that damage is allowed for economic considerations. To facilitate routine elastic design (equivalent lateral load or modal response spectrum analysis), the seismic force at Point E is reduced to that at Point S by a response modification factor, R, for strength design; Point S represents the first significant event (e.g., plastic hinge formation in a beam in a moment frame, or brace buckling in a concentrically braced frame) beyond which the structure responds in the inelastic range (for working stress design, Point E is further reduced to PointWby an Rw factor). When the structure is redundant, with ductility built into members that are expected to undergo inelasticity, the structure deforms further beyond Point S to its maximum strength at Point M and degrades to Point U if strength degradation due, for example, to member buckling or the P-Δ effect, occurs. Therefore, the R factor is mainly composed of two components (Freeman 1990; Uang 1991; NIST 2012).

$$R = R_{\mu}\Omega_{o}$$

where Rμ (¼Ce=Cy) = ductility reduction factor at the system level; and Ωo (¼Cy=Cs) = system overstrength factor. A few observations can be made about the R-factor design procedure:

- The structure is expected to deform into the inelastic range because damage is accepted in a design earthquake for economic reasons;
- The R factor was developed mainly for convenience in routine design because elastic analysis is still valid for structural performance evaluation at Point S;
- Ductility (i.e., inelastic deformation capacity) is needed for structural components expected to experience inelasticity; and
- Ultimate lateral strength at the system level (Point M) can be much higher than that at Point S, where an elastic analysis is performed.

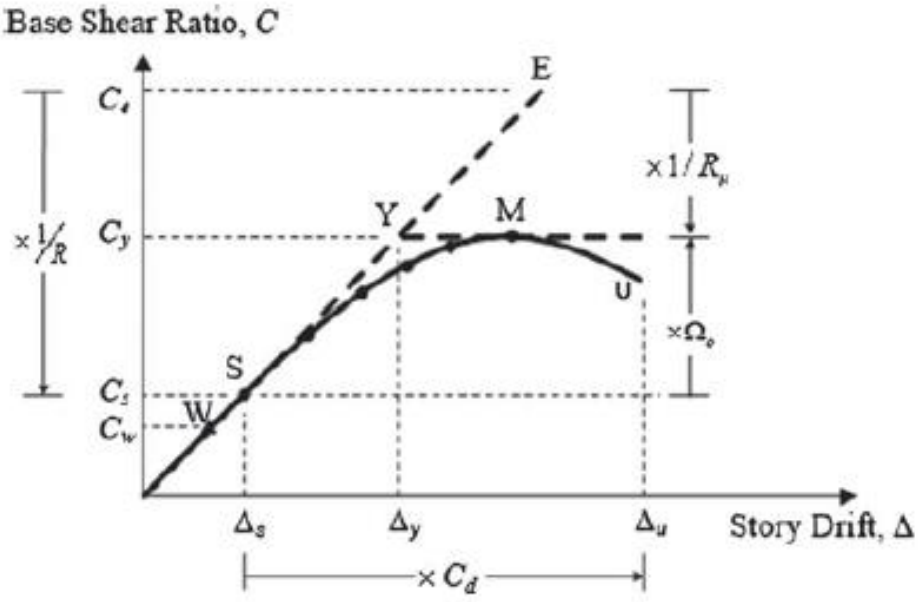

Figure 12 Typical structural response and system performance factors

Regarding the first bullet entry, seismic codes set a target plastic mechanism for each SFRS for energy dissipation that minimizes inelastic deformation demand while maintaining the gravity load–carrying capacity. Taking moment frame design as an example, a classical plastic design may allow plastic hinges to form in either beams or columns if the ultimate strength of the frame is no less than that required. For seismic design, however, codes aim

to achieve a more desirable plastic mechanism that limits the premature formation of story mechanisms by promoting hinging in beams and limiting it in columns. Although the R factor associated with the target plastic mechanism of each SFRS is given in ASCE 7, the designer relies on the AISC Seismic Provisions to ensure that sufficient ductility capacity in the third bullet entry just given is built into these systems. For structural elements that are designed to remain essentially elastic and do not undergo energy dissipation in a seismic event, the fourth bullet entry implies that the horizontal seismic load effect is significantly higher than that computed in accordance with the second bullet entry. The capacity design principles are then used to compute the seismic load effect in these structural components. Because the required seismic forces needed for capacity design correspond to the seismic force level at Point M, conceptually a nonlinear analysis is needed. To bypass nonlinear response analysis for routine design, ASCE 7 uses an empirical overstrength factor, Ωo, to amplify the seismic force effect from Point S to Point M. This amplified effect, equal to the value obtained from the codespecified earthquake load, Eh, multiplied by Ωo and termed Emh, has been specified as not needing to be larger than the value computed from a plastic analysis using the realistic expected values of material strengths, termed Ecl (in 2016 ASCE 7 terminology). Although convenient, multiplying Eh by Ωo has been recognized as flawed because it fails to capture the redistribution of forces that typically occur during nonlinear response and that may affect demands on the elements that are intended to be protected by capacity design principles. Whenever possible, procedures to compute Ecl have been provided in the AISC Seismic Provisions, and in the 2016 edition AISC requires that Ecl, when specified, be used as the value of Emh for capacity design even if it exceeds that computed based on the Ωo factor.

3.3 Pushover Analysis

General earthquake-resistant design (EQ-RD) philosophy, which is widely accepted throughout the world, states that structures are designed to resist low-intensity earthquakes with no damage (structural and non-structural), medium intensity earthquakes with repairable levels of non-structural and structural damage, and high-intensity earthquakes with significant damage to both structural and non-structural elements without overall or partial collapse in order to avoid loss of life. Even though the above EQ-RD philosophy has been targeted to achieve in earthquake engineering society, only the life safety and

collapse prevention in the above general philosophy are explicitly prevented in seismic design codes. Recent earthquake in Turkey and Syria left tens of thousands of deaths and causalities. This phenomenon warns us to work out the performance and response of truss bridges under earthquake. Four different levels and range of seismic performance are defined in evaluating the seismic performance of structures. These four performance levels from high performance to low performance levels are operational level, immediate occupancy level, life safety level, and collapse prevention level, respectively.

Estimating the demands at low performance levels (life safety and collapse prevention levels) requires the consideration of inelastic behavior of the structure. Pushover analysis has been very popular in recent years for performance-based EQ-RD, which is defined as the identification of seismic hazards, selection of the performance levels, and design performance objectives, determination of site suitability, conceptual design, numerical preliminary design, acceptability checks during design, design review, quality assurance during construction, and maintenance during the life of the structure (Vision 2000, 1995). Even though the nonlinear dynamic time history analysis is the best way to compute seismic demands, ATC-40 (1996) and FEMA-273 (1997) proposes to use the nonlinear static procedure (NSP) or pushover analysis for structures in which higher mode effects are significant (Chopra, 2001). In this method, the seismic demands are estimated by nonlinear static analysis of the structure subjected to monotonically increasing lateral forces varying through the height of the structure until either a predetermined target displacement is reached or the structure collapses and base shear vs. roof displacement of the buildings is obtained, which is generally called capacity curve.

This capacity curve is a valuable tool for study of global behavior of structures. Since realistic material response is used in mathematical modeling, the results will be close to those expected during the design earthquake. The two key steps in applying this method, lateral force distribution and target displacement, are based on the assumption that the response of the structure is mainly from the fundamental mode and that the mode shapes remain unchanged after the structure gets into the inelastic region. The validity of the assumed lateral force distribution after the structure gets into the inelastic region and how close are the results obtained from the pushover analysis to the nonlinear dynamic time

history analysis are questionable. It is implicitly assumed in pushover analysis that seismic demands computed at the target displacement are close approximations of the maximum seismic demands during the design earthquake. It should also be noted that pushover analysis corresponds to monotonically increasing lateral loading, which does not take into account reduced strength due to cumulative damage.

3.4 Design Data and Modelling

Firstly, some necessary data are prepared for proposed bridge. Modified Warren truss with verticals is selected for main truss: ten divisions are spaced 12 meters which makes 122 meters simply supported span. Two 3.8 meters wide traffic lanes are located on each direction and 1 meter wide side walk is also attached on each side. The slope of main diagonal members is designed to get 60 degree with bottom chord.

3.4.1 Warren Truss History

Bridge historians and early textbooks generally call a truss with alternating compression and tension diagonals a Warren; however, sometimes it is called an equilateral truss since all panel lengths and diagonals are of equal length creating a series of equilateral triangles. When the panel lengths are shorter than the equal length diagonals, it was sometimes called an isosceles or isometric truss.

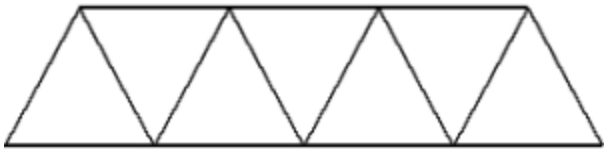

Figure 13 Commonly accepted Warren Truss.

When the span length increases and the height of the truss necessarily increases, the long compression members in the top chord need bracing to minimize buckling in the vertical direction. In this case, verticals are placed from the lower chord panel points up to the mid point of the chord member directly above. In addition, the deck structure stringers get longer requiring either heavier members or the addition of verticals from the top chord panel points dropping down to shorten panel lengths.

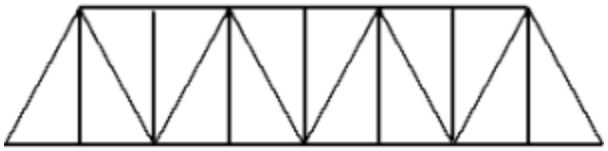

Figure 14. Warren Truss with verticals to support top chord and deck structure.

Neither of these truss styles are what James Warren and Willoughby Monzani patented in 1848 in England. They based their patent on similar trusses that were built in France by Alfred H. Neville and a patent that was granted in England to William Nash in 1839 on a similar design. Warren and Monzani were well known English engineers, and their design was for a truss that could be used as a deck or a through truss. They used cast iron for the top chord, and diagonals and wrought iron bars and links for the lower chord members. The top chord cast iron members were connected through cast iron junction blocks, and the cast iron diagonals and lower chord wrought iron members were connected with pins. The title of the patent application was Construction of Bridges and Aqueducts and was issued on August 15, 1848 with Patent #12,242. Their profile was rectangular. Even though Squire Whipple in the United States had published the method of determining loads in truss members under uniform and varying loads, this method had not made its way to England. It wasn't until 1850 that W. B. Blood developed a method of analyzing triangular trusses, as Whipple had.

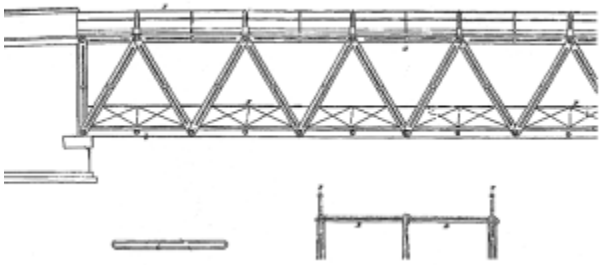

Figure 15 Warren and Monzani patent drawing showing deck at both levels.

3.5 FEM Model Geometry

The double Warren truss is selected to provide an adequate lateral bracing to the bridge on the top and bottom. Sway bracing is also considered to get a safe lateral stability of the structure. Load consideration is based on *AASHTO specifications and HS 20-44* is considered as design truck. General view and finite element model of the steel truss bridge are described in Fig.16 and 17 respectively.

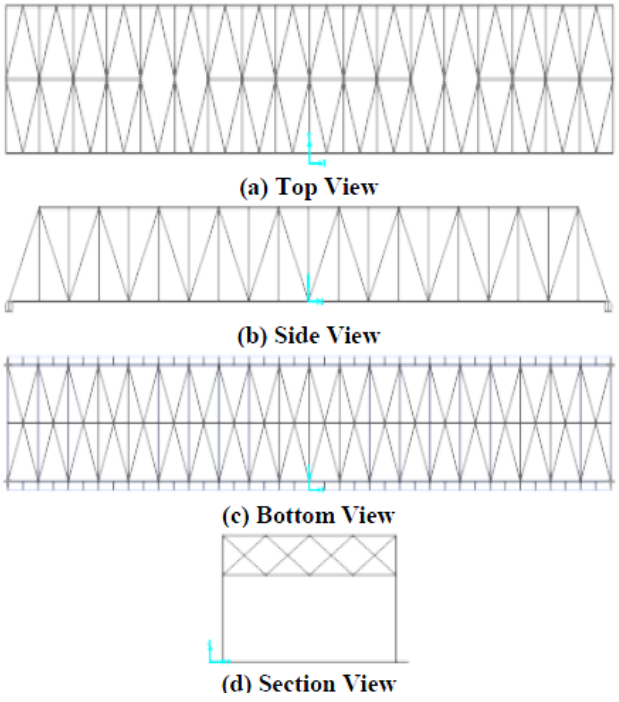

Figure 16 General view of steel truss model

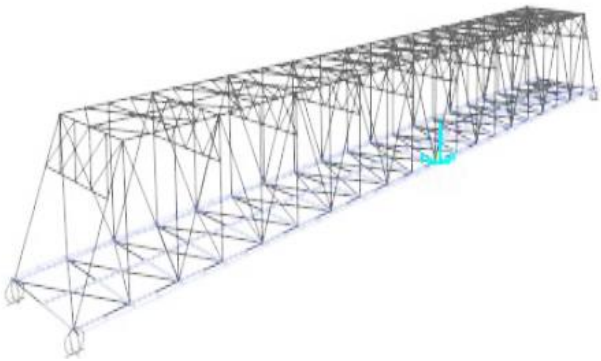

Figure 17 General view of steel truss model

3.6 Design data of the proposed model

The following Table2 shows the description of the proposed model and design data used in this model:

Table 2 Design Data of Proposed Bridge

Item	Description
Truss Type	Modified Warren Truss with Verticals
Number of Divisions	10
Division Length	12 m
Bridge Height	10 m
# of Lanes	4
Lane width	4 m
Side Walk Width	1 m
Span Length	120 m
Design Truck	HS20-44
Design Speed	60 mph

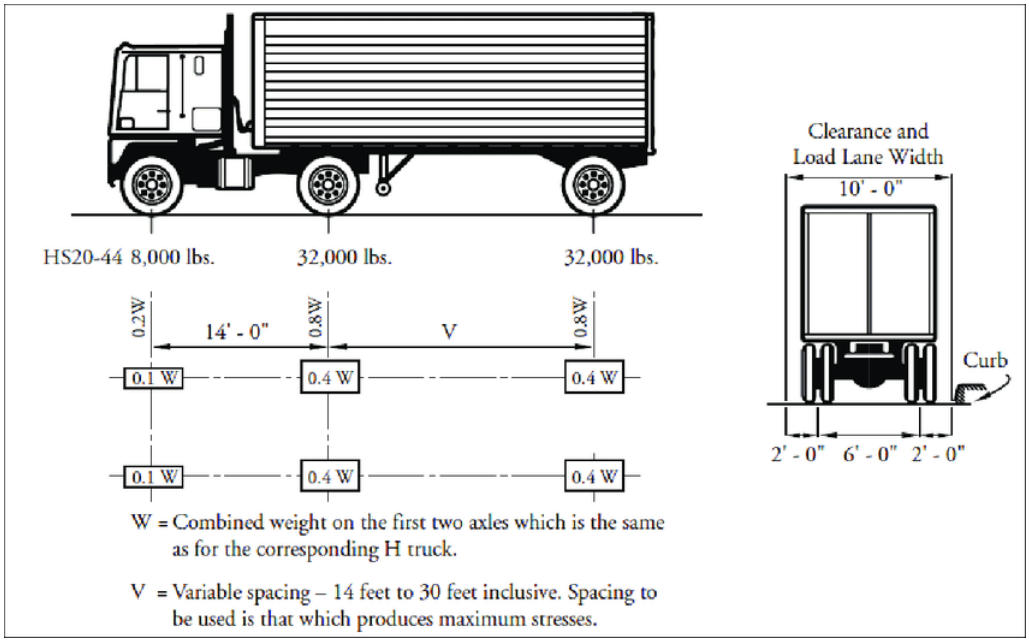

Figure **18** HS20-44 Loading

3.7 Material Properties of the proposed model

The following Table 3 presents the material properties (Concrete and steel) which will be adopted in the model:

Table 3 Material Properties of the Proposed Bridge

Item	Value
1. Analysis Properties Data	
Concrete weight per unit volume	25 kN/m3
Steel weight per unit volume	2400 kg/m2
Modulus of Elasticity of Concrete, Ec	30 GPa
Modulus of Elasticity of Steel, Est	200 GPa
Poisson's ratio of Concrete, Uc	0.2
Poisson's ratio of Steel, Ust	0.3
Shear Modulus of Concrete, Gc	10 GPa
Shear Modulus of Steel, Gst	75 GPa
Thermal Expansion factor of Concrete, Ac	$10 \times 10{-}6/°C$
Thermal Expansion factor of Steel, Ast	$1.2 \times 10{-}5/°C$
2. Design Properties Data	
Shear Reinforcement yield stress fys	350 MPa
Bending Reinforcement yield stress fy	350 MPa
Concrete Compression stress Fc'	24 Mpa
Minimum yield stress Fy	480 MPa
Minimum tensile stress Ft	620 MPa

3.8 Loads on the bridge

All of the structure including bridges must be designed to resist the various kinds of loads such as gravity as well as lateral loads. There are many kinds of load effect on structure. Every kinds of load are depending on duration, direction of action, types of deformation and nature of structural action. The loads considered on this bridge are dead load, live load including wind load based on ASCE7-05, temperature load according to AASHTO and seismic load according to UBC-97.

Dead load shall include the self-weight of the superstructure consisting of the deck (including the wearing surface), sidewalks, curbs, parapets, railings, the supporting stringers, and floor beams. For the proposed bridge, dead loads are considered according to AASHTO-LRFD specifications:

- *Unit weight of concrete = 25 kN/m3*

- *Unit weight of asphalt = 2.2 t/m3*

-*Weight of hand rail = 3 kN/m*

Live loads refer to loads due to moving vehicles that are dynamic, i.e., loads that change their position with respect to time along the entire span. Live loads can be divided such as: truck loads, lane loads and sidewalk loading. Live loads are considered according to AASHTO-LRFD specifications:

- *Pedestrian live load = 4 kN/m2*

- *Vehicular live load = HS 20-44*

- *Impact load, I = 50/(L+125)*

According to ASCE7-05, the determination of wind design force on a structure is basically a dynamic because gusts and other aerodynamic forces will continually affect a bridge.

- *Exposure type = Type C*

- *Basic wind velocity = 100 mph*

- *Important factor = 1.15*

- *Gust factor = 0.85*

- *Pressure coefficient = 0.8 inward*

- *Pressure coefficient = 0.5 outward*

An earthquake consists of horizontal and vertical ground motions, with vertical motion usually having much the smaller in magnitude. Earthquake loading is considered according to the UBC-97.

- *Seismic zone = 4*

- *Seismic zone factor, Z = 0.40*

- *Soil profile type = Sc*

- *Seismic important factor, I = 1.25*

- *Over strength factor, R = 8.50*

In general, thermal effects are caused by the fluctuations in temperature and caused by the structural redundancies or bearing failures. In this paper, the temperature difference of 16°C, 10°C and 10°C in X, Y and Z direction of each element respectively.

According to AISC-LRFD specifications, three limit states (strength, service and extreme event) are selected to perform the analysis and design procedure. The considered limit states are as follows:

i. Strength IIII limit state (Str. III)

ii. Extreme Event I limit state (EE. I)

iii. Service I limit state (Ser. I)

3.9 SAP 2000

SAP2000 is an extremely versatile and powerful program, with many features and functions, The top menu line contains all of the commands and options available to SAP2000, including Define, Draw, Select, Assign, Analyze, Display and Design. In addition to these menus, many of the most frequently used commands are accessible as a single click button in the screen regions surrounding the drawing areas. The availability of a button is indicated in the main menus by the existence of an icon to the left of the command. The lower right corner shows the current unit selection. Figure 19 shows the layout of the interface.

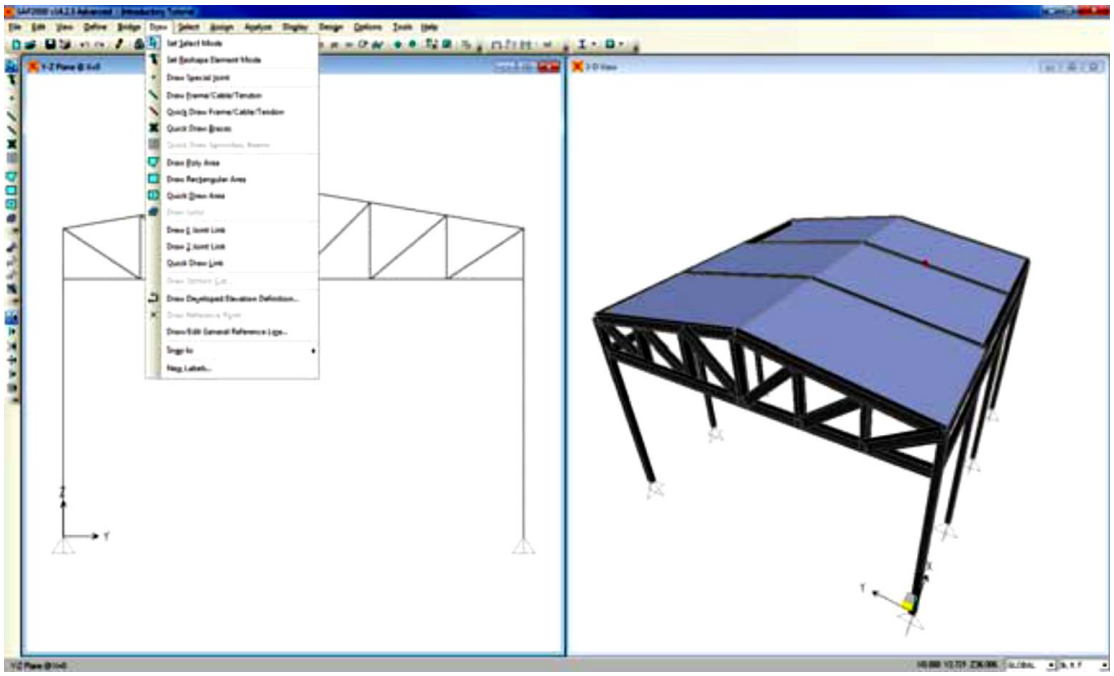

Figure 19 Main Interface of Program

One of the main important steps is how to define the sections, the following figures show how to define the sections:

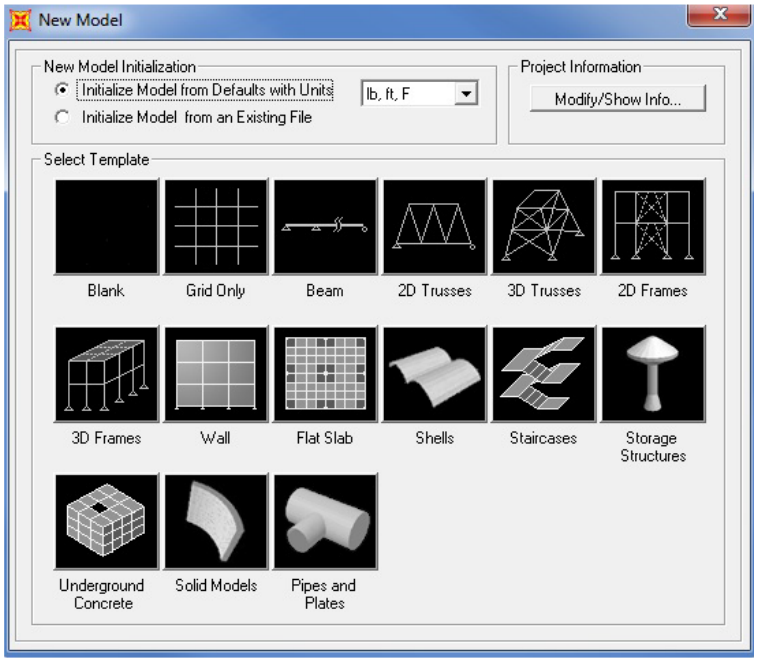

Figure **20** Sap 2000

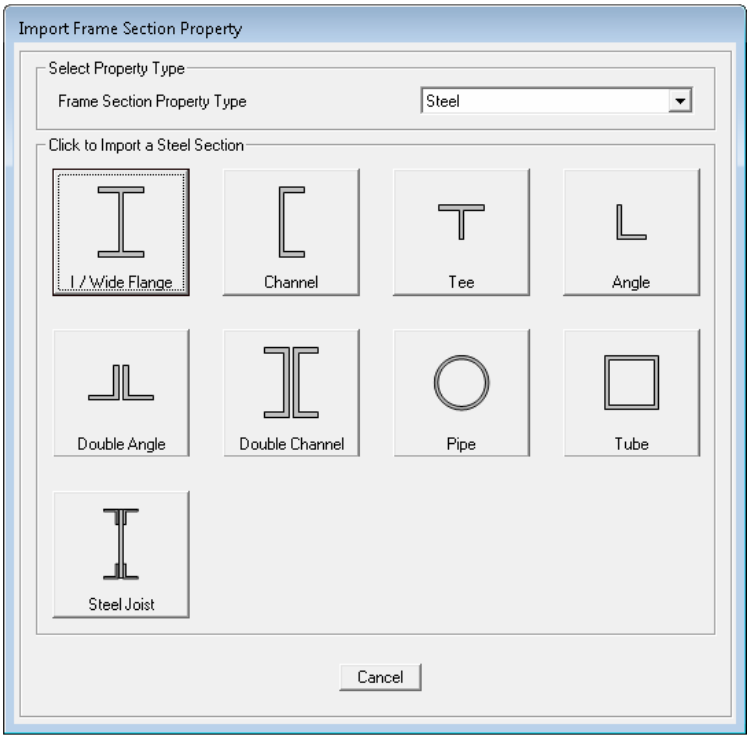

Figure 21 New sections

Verify that Steel is showing in the Frame Section Property Type drop-down list, and then in the Click to Import a Steel Section area of the Import Frame Section Property form, click the Tube button, which will open the Section Property File form.

Section List:

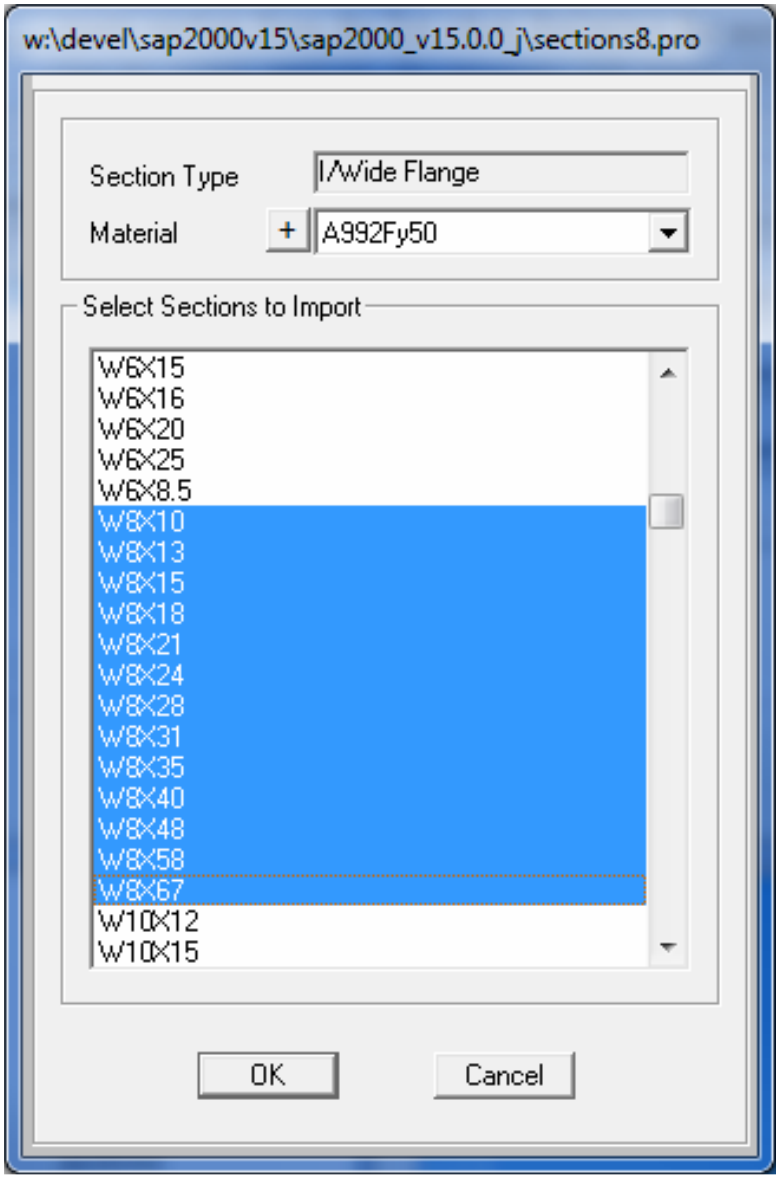

Figure 22 Import sections

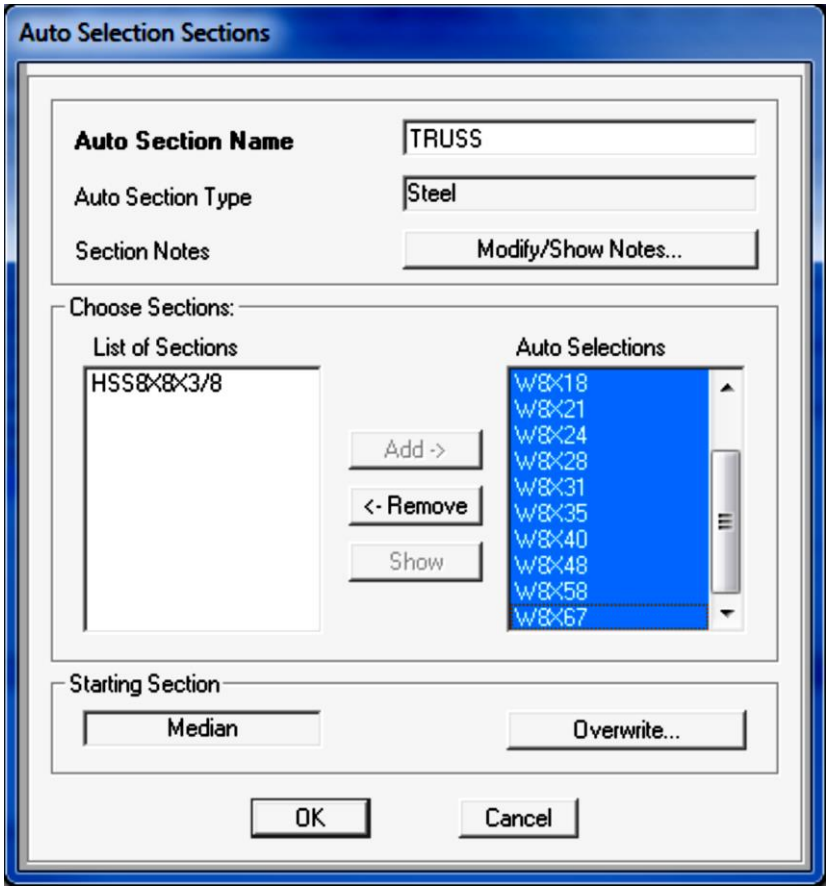

Figure 23 Import Auto selection sections

Chapter 4: Results and Analysis

4.1 Analytical Results and Discussion

After simulating the proposed model bridge with loading combination and moving load case, the results including the axial force (P), torsion (T), shear about vertical and horizontal axis (V2), (V3), moment about vertical and horizontal axis (M2) and (M3), for static case, are obtained as shown in the following figure 24:

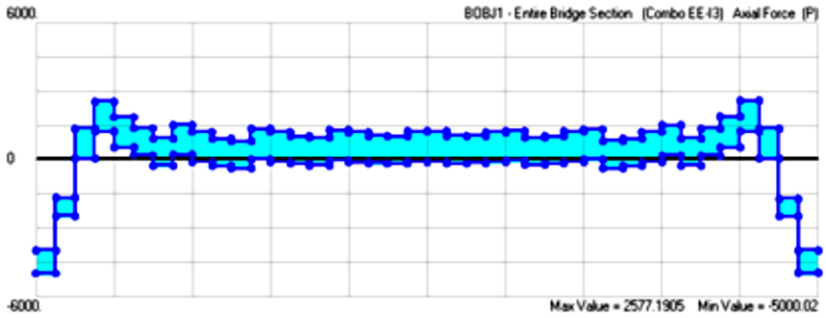

Figure 24.a Axial Force (P) distribution on entire bridge.

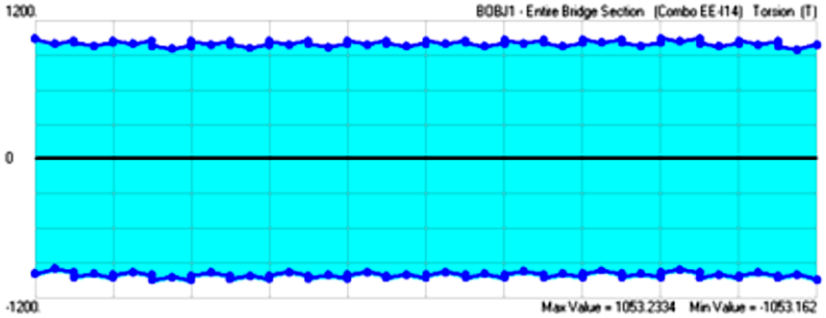

Figure 24.b Torsion diagram for entire bridge.

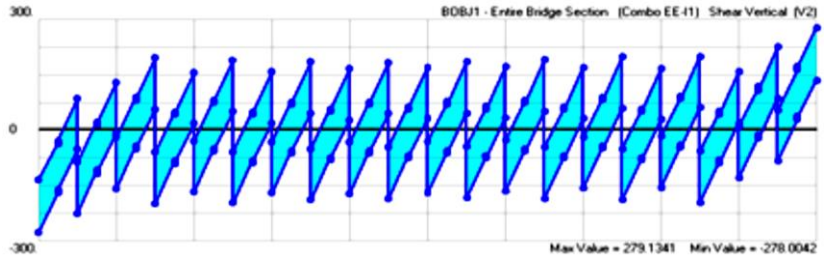

Figure 24.c Shear force (V2) diagram for entire bridge.

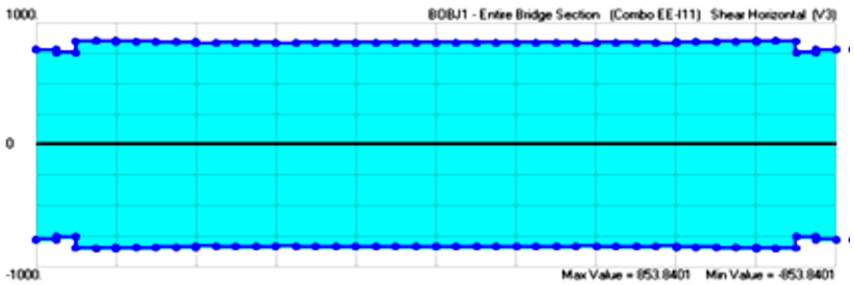

Figure 24.d Shear force (V3) diagram for entire bridge.

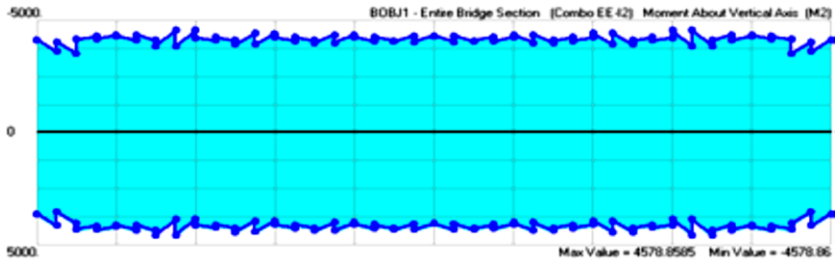

Figure 24.e Moment (M2) diagram for entire bridge.

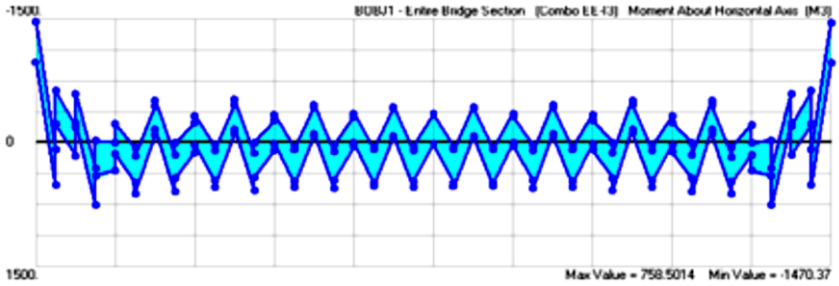

Figure 24.f Moment (M3) diagram for entire bridge.

Figure 24 Axial Force, Torsion, Shear and Moments for the entire bridge

According to AISC-LRFD specifications, deflection check for the bridge is carried out. Allowable Deflection:

$$\Delta_{all} = \frac{l}{600}$$

$$\Delta_{all} = \frac{120}{600} = 0.2\ m\ \ (20\ cm)$$

Maximum deflection due to dead load = 5.88 cm less than allowable deflection value then it is ok. Table 4 presents the designed sections for all members is less than allowable deflection:

Table 4 designed sections

Item	Section
Top Chord	W 14×450 to W 14×550
Bottom Chord	W 14×90
Diagonal Members	W 14×90, W 14×550
Vertical Members	W 14×176
Top Longitudinal Members	W 14×90
Top Lateral Members	W 14×74
Top brace elements	W 14×43 to W 14×61
Sway brace elements	W 12×19
Sway lateral Members	W 14×90
Portal Members	W 12×30
Floor Beams	W 14×145
Bottom Brace Elements	W 12×40
Bottom Longitudinal Members	W 12×30

The stress distribution and forces on the bridge is nearly symmetric as the action of a simply supported span bridge. And, due to the truss action, top chord members suffer from compression and the heavier weight is needed for stronger stiffness while bottom chord members can be designed with a lighter section. The stress distribution on the truss elements can be controlled by using vertical members. The stiffer the vertical members are, the lighter the diagonal elements. During the design process, it is found that diaphragm effect is significant on the stability and rigidity of the structure. It makes no displacement monitored under pushover analysis as a result of very rigid and strong truss structure in some condition. Therefore, the use of diaphragm effect on the truss bridge should be widely considered for the desired analysis. The stress distribution on the entrance and exist of the bridge is significantly higher than on the mid portion. But the section weight of the floor beams on the end portions can be design lighter than that of the mid portions as the traffic loads is not fully distributed on these sections. On the hinge restraint support, the effect of torsion due to service loads is considerably higher than that of the effect on the other side.

Figure 25 presents the pushover curve obtained by the later earthquake in traverse direction. Target displacement, 40 centimeters (4% of the bridge height) is selected to perform the analysis.

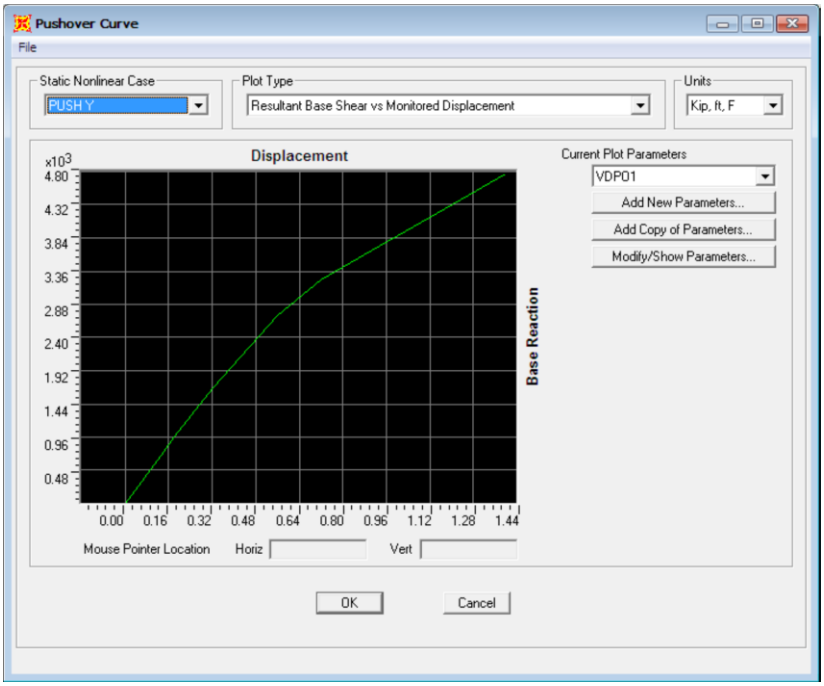

Figure **25** Pushover Curve

Figure 26 shows that capacity and demand curves are intersected in immediate occupancy zone. This point of intersection is called performance point. Based on this performance point location the damage intensity can be calculated. Above green line (pushover curve) is divided into three stages, i.e. immediate occupancy, life safety, collapse prevention. If this point located in immediate occupancy state, the damage intensity is light and, if the performance point lies in life safety, the damage intensity is moderate. Similarly, if performance point lies in collapse prevention, then damage intensity is severe.

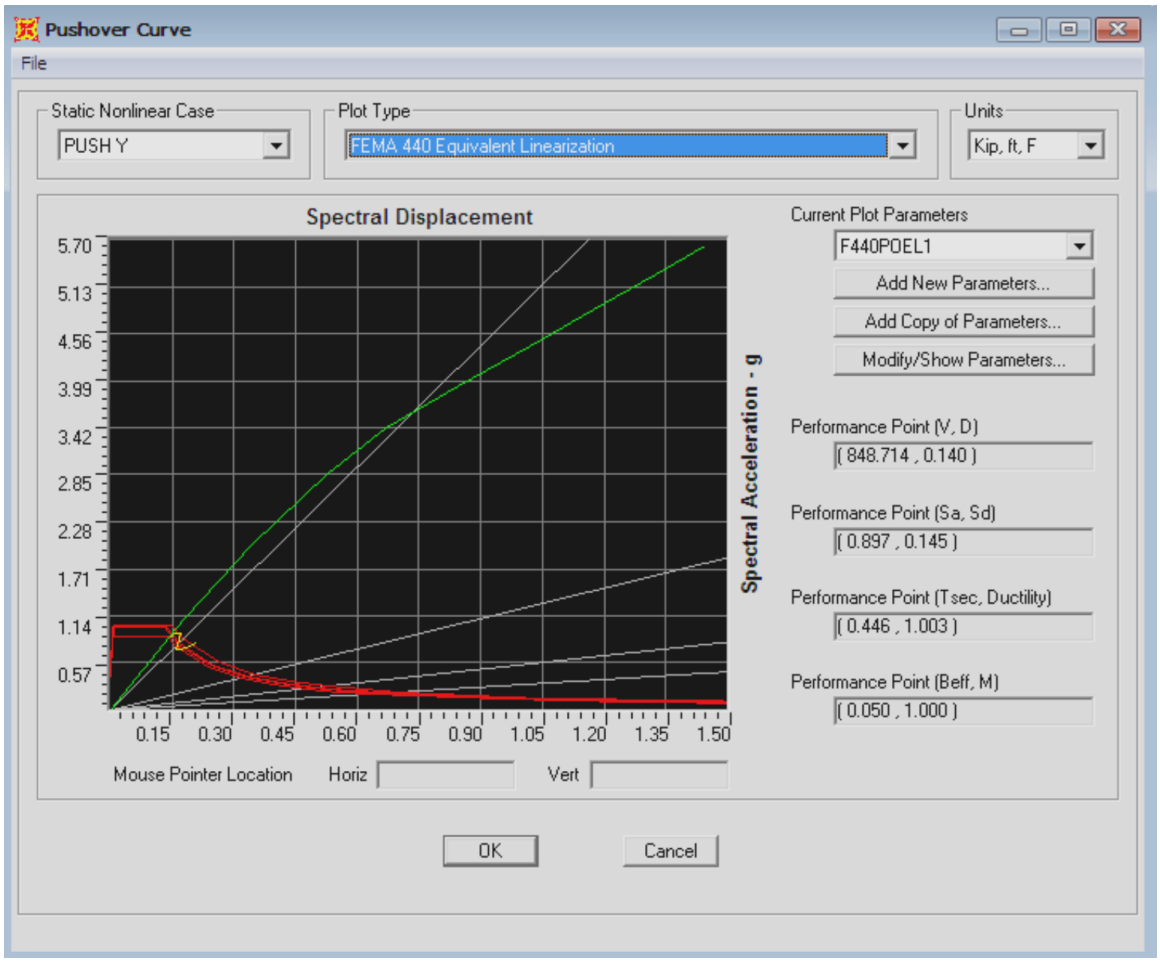

Figure 26 Pushover curve according to FEMA 440 equivalent Linearization.

The following Table 5, presents the damage levels:

Table 5 Damages Levels

Description	Symbol	Illustration
B		Structures can operate normally. This Performance Level (PL) are expected to sustain minimal or no damage to their structural and non-structural components.
IO		This performance level is expected to sustain minimal or no damage to the structural elements and only minor damage to the non-structural components. While it would be safe to reoccupy a structure meeting this target PL immediately following a major load.
LS		Structures meeting this level may experience extensive damage to structural and non-structural components. Repairs may be required before preoccupancy of the structure, and may be deemed economically impractical.
CP		Little residual stiffness and strength and large permanent drifts occurred. Some exits were blocked and the structure nearly collapses.
C		The maximum limit in the structure withstand the major loads.
D		The structure is not able to withstand the lateral loads but it was still able to withstand the force of gravity.
E		The structure is damage

Target of displacement

Target of displacement of the bridge structure should be determined earlier before starting the nonlinear static analysis. The following Equation is used to calculate the target of displacement:

$$\delta_T = C_0 C_1 C_2 C_3 S_a \left(\frac{T_e}{4\pi} \right)^2 g$$

where:

C0 = modification factor relates the spectral displacement and the roof displacement. the value of C0 is 1.0.

C1 = Modification factor to relate expected maximum inelastic displacements to displacements calculated for a linear elastic response, where the value of C1 is 1.0 if Te ≥ TS.

C2 = Modification factor to represent the effect of pinched hysteretic shape, stiffness degradation and strength deterioration on the maximum displacement response, where C2 is 1.0.

C3 = Modification factor to represent increased displacements due to dynamic P-Δ effects. For the structure with positive post-yield stiffness, shall be set equal to 1.0.

Sa = Response spectrum acceleration, at the effective fundamental period and damping ratio of the building in the direction under consideration.

Te = The effective fundamental period, the value of Sa obtained from the equation bellow:

Sa = CD x S0 = 0.92 x 1.2 = 1.104.

The target displacement of the bridge models can be seen in Table 6.

Table 6 Calculated Target Displacement Values

Model	**Target Displacement (cm)**
A model	10.31
B model	7.34
C model	2.72
D model	20.19
E model	11.03
F model	6.96

The plastic hinge formation due to traverse lateral load is presented on table. The first plastic hinge formation is obtained on the sway braces on step 1, in immediate level.

Table Display

File Edit

Pushover Curve - PUSH Y

Step	Displacemer	BaseForce	AtoB	BtoIO	IOtoLS	LStoCP	CPtoC	CtoD	DtoE	BeyondE	Total
	in	Kip									
0	3.984E-13	0.000	824	0	0	0	0	0	0	0	824
1	1.680000	845.836	820	4	0	0	0	0	0	0	824
2	2.111287	1061.862	808	12	0	0	0	4	0	0	824
3	3.984775	1884.754	768	6	3	0	0	47	0	0	824
4	6.212163	2712.674	746	20	4	0	0	54	0	0	824
5	7.926877	3230.383	728	22	8	0	0	66	0	0	824
6	9.918888	3691.667	728	18	8	0	0	70	0	0	824
7	11.925113	4152.826	728	18	8	0	0	69	0	1	824
8	13.989522	4629.561	728	18	8	0	0	67	0	3	824
9	15.749995	5040.382	728	18	8	0	0	63	0	7	824
10	16.800000	5285.599	726	20	8	0	0	59	0	11	824

Current Sort String

Current Filter String

Done

Figure 27.a : Plastic Hinges Results

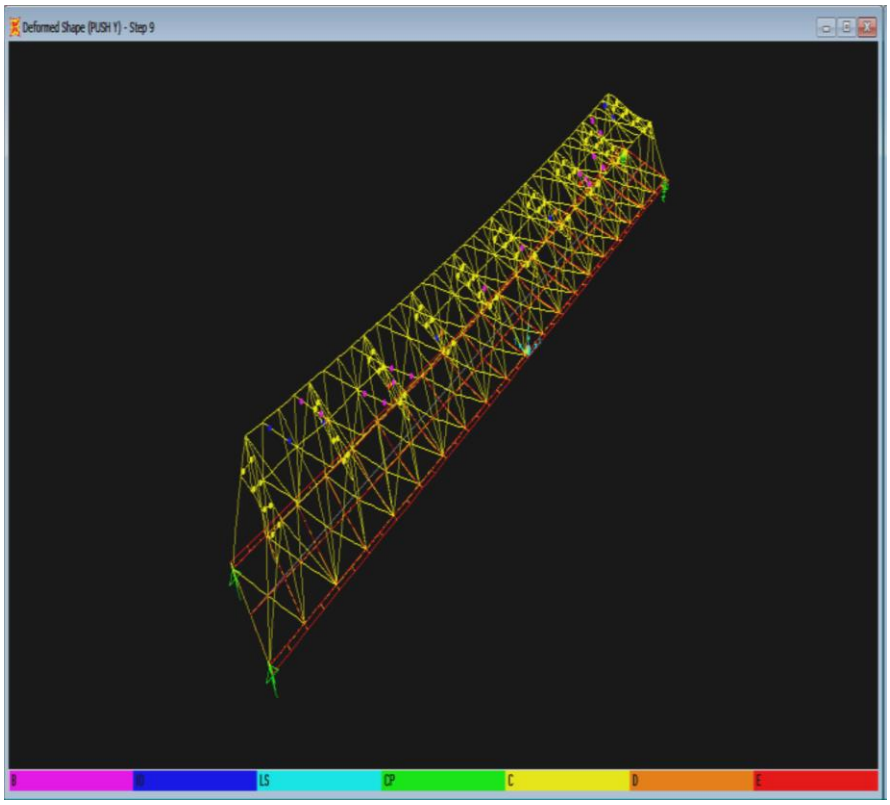

Figure 27.b : Plastic Hinges Formation at step 9

Figure 27 Plastic Hinges in the bridge

On step 2, these four hinges overcome to collapse prevention level and next twelve hinges can be seen in immediate level. For step 7, one of the plastic hinges totally collapse. The formation of plastic hinges starts on sway brace and propagate to top braces near support and finally yielding on portal braces is observed. The hinges formed in portal braces are beyond the collapse prevention level on step 10 which is in danger zone. On the top brace, some hinges are founded out in the life safety level. Plastic hinge result and Plastic Hinges formation on step 9 shown in figure 27.

4.2 Parametric study of Ductility of bridge models

Different models with different target displacements and different performance levels are proposed, Target displacement of the A-model is 10.31 cm as illustrated in Table-6. The performance level of the structure is at the boundary of Immediate occupancy (IO). The IO means no damage to structural components and can be used immediately. The target displacement exceeded at step 1. The first yielding occurred at the bottom of the diagonal chord at the end frame. In step 3 as drawn, it reached a performance level which is occurred at the upper of the diagonal chord at the end frame. In step 12, the top of diagonal chord at the end frame was collapse, and the tensile diagonal chord near S2 and S3 supports are applied a plastic hinge.

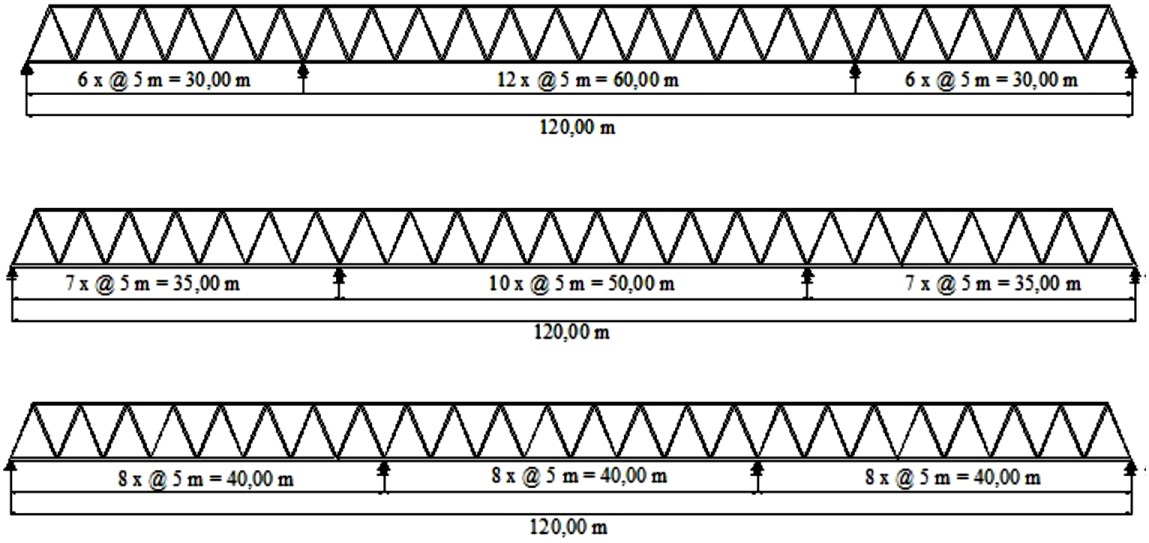

Figure 28 A, B and C models geometry

In B-model, bridge has nearly the same dimension as A-model which expressed the center span of 50 m. Target displacement of the B-model is 7.34 cm. Afterwards, it is compared to the first step data which has been passed through the value of target displacement. The performance level of the structure is still at the boundary of B - IO. The structural components are implied no damage and could be used immediately as well. The first yield occurred at the bottom of diagonal chord imminent to S2 and S3 supports. From that condition, this model has given a similar result as previous model. In that case, the differences of span ratio of this model should be evaluated smaller than 50 m. The further condition, the bridge C-model is presented the same variety of span length which is allocated 40 m for both center span and side span.

In C-model, the target is 2,72 cm. That value become a compulsory parameter that should be managed. Collapse processes is evaluated by both data as well. Furthermore, the bottom chord at support S2 and S3 become yield in tension at first. Then, the upper chord become yield in tension in the following as well. In that matter, the structural performance level of its structure has been reached. Next, compression yield appeared near the intermediate frame in area of the span center. Finally, after reaching the performance level, the structure is collapse. The diagonal member fully damaged near the S2 and S3. The maximum tension happened when the increment loading increases. One of the spans sharply fell underneath and one another is upraised because of the damage at support S2 and S3.

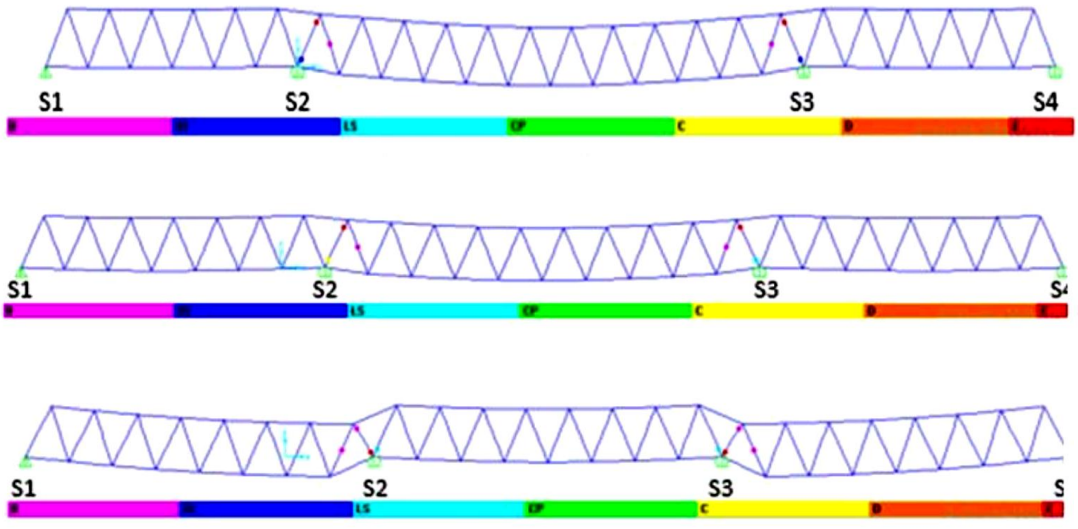

Figure 29 Collapse for A, B and C models

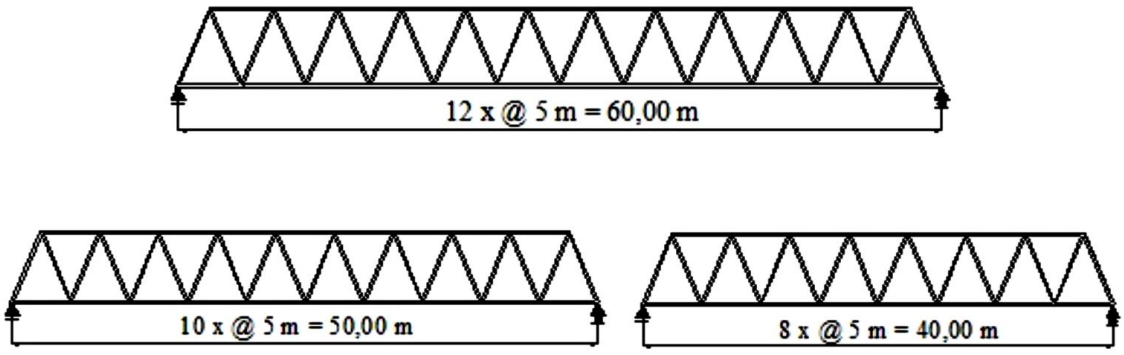

Figure **30** D, E and F models geometry

The other models will be used in this study are single span models which is given a shorter step evaluation than previous models. It is also given a simple prediction of collapse condition which will be happened at the center of the span. The allowable displacement is 20,19 cm. In fact, both data of analyses are considered and it is shown that performance level of the structure is fulfilled at the boundary B-IO. There is no damage to the structural component which is well-considered to be used shortly.

D-model case with 60 m length. First condition, the upper chords at the span center become yield in tension. It is illustrated by the implied purple color on the truss, i.e. A-B. Then, second condition, when the load amplification is reached the performance level, the color point is changed to be in ultimate strength condition, specifically B-IO to C-D. Finally, the third condition, the maximum tensile strain is occurred by the loading mechanism. The failure is located in the same center of span that leads significant damage on the structure (collapse).

In E-model, the total length of the span is allocated 50 m. The target displacement is also considered of 11,03 cm. The comparison is implied that the performance structure is at the boundary B-IO. As the matter of fact, there is no concerned damage of the structural components. The structural system could still be used immediately. The failure is almost given a typical condition with the D-model. The upper chords at the span center became yield in tension at first. Finally, when the load amplification reached, the upper chord buckled at the span center is in the performance level in B-IO to C-D condition. Then, the

maximum tensile strain at the upper chord is collapse in the further. The failure is located in the same center of span that leads a further damage or collapse on the structure.

In F-model, the total length of the span is changed to 40 m length. It is also implied the difference of target displacement of 6,96 cm. The result shown that the performance level occurred at the boundary B-IO as well.

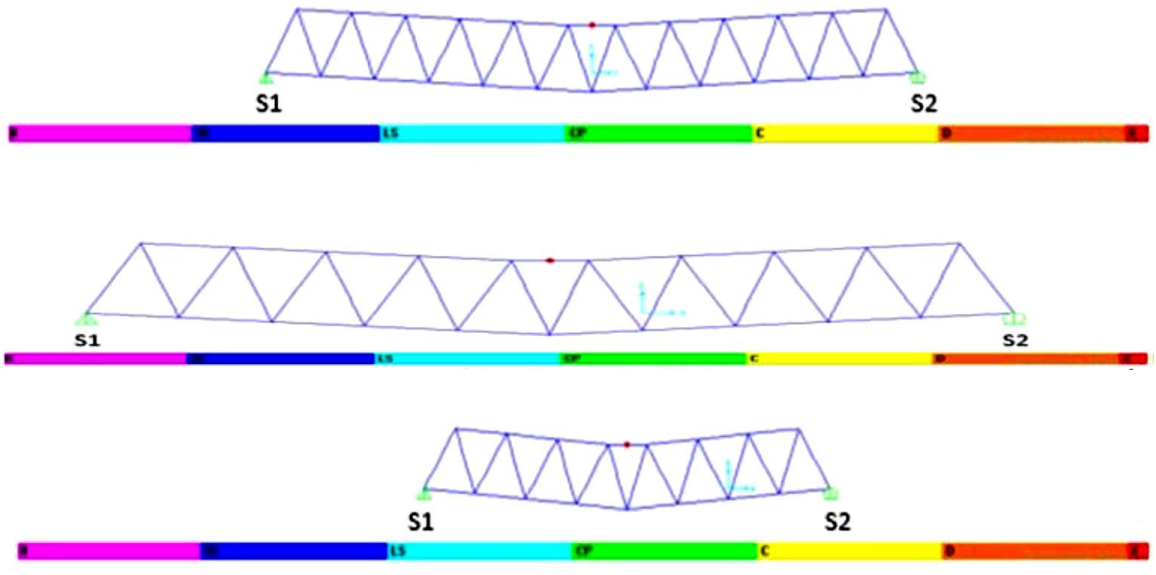

Figure 31 Collapse for D, E and F models

The failure mechanism and the plastic hinge characteristic due to performance level. The value of F-model is declined as the smallest according to displacement and base shear force. The upper chords at the span center became yield in tension at first with 12.39 cm displacement. Finally, when the load amplification reached at 325.75 t, the upper chord buckled at the span center is in the performance level in B-IO to C-D condition. Then, the maximum tensile strain at the upper chord is collapse in the further with 20.11 cm displacement. The failure is located in the same center of span that leads a further damage or collapse on the structure.

4.2.1 Ductility evaluation

Ductility describes the extent to which a material (or structure) can undergo large deformations without failing. The term is used in earthquake engineering to designate how well a building will endure large lateral displacements imposed by ground shaking. The ductility of each bridge models can be calculated from the curve capacity. The following equation is used to calculate the ductility of the bridge:

$$\mu = \frac{\delta_u}{\delta_y}$$

μ *=ductility*

δ_u *=the displacement at the ultimate point*

δ_y *=the displacement at the first yield point*

Damaged or collapse analysis was conducted for the two bridge models with different span ratios. It presents that collapse process and deformation depend on the span ratio. In this section, ductility of the two bridge models is evaluated as shown in Table-7. The ductility index μ of bridge is increased respectively from A to C and from D to F. In A-model, it is given the smallest value due to base shear force and ultimate point event all A-models have the typical length. The opposite condition is presented by D-model is plotted to have the smallest value of both base shear force and ultimate point.

The comparisons of the ductility of the models were no significant differences, the reason is each model using the optimum section members for the truss bridges. The actual ductility of the models already met the requirements of standard.

Table 7 Ductility of All models

Model	Base Force (T)		First Yield	Ultimate Point	Ductility index
	First Yield	Ultimate Point	δ_y	δ_u	μ
A	601.3	653.9	14.80	15.35	1.04
B	980.03	1047.31	9.92	10.35	1.05
C	217.91	246.56	3.16	3.24	1.07
D	133.11	144.07	23.91	25.25	1.06
E	374.70	387.71	18.06	19.15	1.07
F	315.22	325.75	12.39	13.23	1.09

4.3 Nodes Displacements

Model F was chosen to perform a parametric study to investigate the vertical and horizontal displacement for both vertical and horizontal earthquakes, all nodes were chosen on the upper chord of the steel truss bridge, the displacements are shown in the table 8 below, Figure 32 presents the F model with the chosen nodes. The displacement values given in Table 8 summarizes the displacement values recorded when the ultimate strain values reached in the steel members which represents the failure scenario.

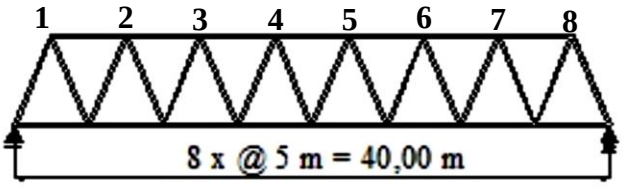

Figure **32** Nodes nomination at model F

Table 8 Displacement values recorded when the ultimate strain

Node #	#1	#2	#3	#4	#5	#6	#7	#8
H. EQ Disp. (mm)	1.12	2.99	8.26	12.25	13.20	9.02	3.14	1.01
V. EQ Disp. (mm)	0.022	0.95	3.22	9.53	10.11	4.52	1.11	0.12

The highest displacement value was found at node # 5, the horizontal EQ gave higher displacement values than the vertical one with difference between horizontal and vertical earthquake values = (13.20-10.11)/10.11 = 30 % difference

4.4 Yield strength effect

The previous model F was used to create a parametric study of yield stress effect on displacement values, three different Fy values were used, 235, 350 and 480 MPa. The different displacement values are shown in the following figure 33. The ultimate displacement values at the nodes of the steel truss structure increases when the yield stress of the steel used decreases.

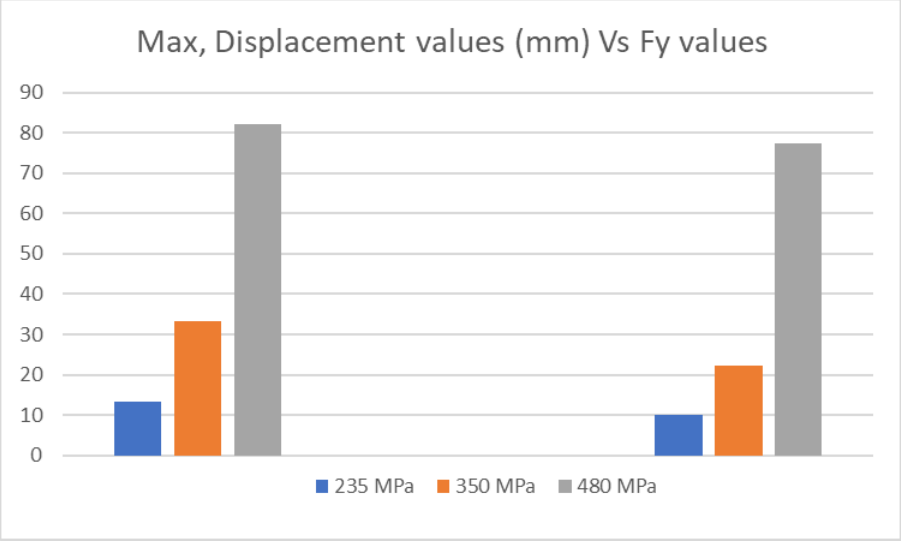

Figure 33 Maximum Displacement Values (mm)

Chapter 5: Conclusions and Recommendations

5.1 Conclusions

The conclusion of this thesis is taken based on the nonlinear static Pushover analysis using SAP 2000. The following conclusions were obtained as follow:

- For performance-based design, the pushover analysis is shown to be a useful tool for determining inelastic strength and deformation demands and for exposing design weakness.
- In this thesis both capacity and demand curves are intersected below immediate occupancy zone. Such that slight damage will be formed when subjected to pushover loads in seismic Zone-IV.
- Plastic hinges formation starts on diagonal truss members then propagates to hangers and posts. From this study, it can be seen that sway braces are critical for traverse lateral load and top braces near supports and portal braces should be designed carefully for traverse lateral loads. For longitudinal lateral loading, diagonal members at the mid-span should be stiffer than other parts of the structure. Hangers and posts need adequate strength for both lateral loads.
- The first collapse of the continuous steel truss bridge is in the diagonal chord of the end of frame. While the first collapse of the single steel truss bridge models occurred in the upper chord at mid-span.
- The level of performance of all models are in the IO, which means there are no damage to the structural components and the structures can be used immediately after excessive or sudden loads.
- The actual ductility to all models of the bridges already met the requirements of standard, the ductility is about 1.07. These results could not show the comparison of the ductility of the models because of each bridge model using the optimum section members, even the bridge models have difference span length.
- The highest displacement value was found when the horizontal EQ applied with difference between horizontal and vertical earthquake values = 30 %
- The ultimate displacement values at the nodes of the steel truss structure increases when the yield stress of the steel used decreases. The maximum displacement value exceeded 80 mm when Fy=235 MPa.

5.2 Recommendations and Future Work

The following points can be appointed for further research in this area:

- The non-linear behavior of the material to be considered in the FE modelling, so a Time-History Non linear dynamic FE analysis is highly recommended.
- A parametric study which takes into account both geometry and seismic factors are recommended to be studied in further studies.
- One of the main important points that can be taken into account in future studies, is taking different loading types rather than the HS20-44 truck.

REFERENCES

Baer, G., Sandwell, D., Williams, S., Bock, Y., Shamir, G., 1999. Coseismic deformation associated with the November 1995, Mw= 7.1 Nuweiba earthquake, Gulf of Elat (Aqaba), detected by synthetic aperture radar interferometry. J. Geophys. Res. Solid Earth 104, 25221–25232.

Ben-Avraham, Z., 1985. Structural framework of the gulf of Elat (Aqaba), northern Red Sea. J. Geophys. Res. Solid Earth 90, 703–726.

Ben-Avraham, Z., Schubert, G., 2006. Deep "drop down" basin in the southern Dead Sea. Earth Planet. Sci. Lett. 251, 254–263.

Boore, D.M., Joyner, W.B., Fumal, T.E., 1997. Equations for estimating horizontal response spectra and peak acceleration from western North American earthquakes: A summary of recent work. Seismol. Res. Lett. 68, 128–153.

Buckle, I., 2006. Seismic Retrofitting Manual for Highway Structures: Bridges. Federal Highway Administration, Office of Research, Development and ….

Calvo, R., 2002. Stratigraphy and petrology of the Hazeva Formation in the Arava and the Negev: Implications for the development of sedimentary basins and the morphotectonics of the Dead Sea Rift Valley. Isr Geol Surv Rep GSI2202.

Cardone, D., 2007. Nonlinear static methods vs. experimental shaking table test results. J. Earthq. Eng. 11, 847–875.

Causevic, M., Mitrovic, S., 2011. Comparison between non-linear dynamic and static seismic analysis of structures according to European and US provisions. Bull. Earthq. Eng. 9, 467–489.

Choi, E., Jeon, J.-C., 2003. Seismic fragility of typical bridges in moderate seismic zone. KSCE J. Civ. Eng. 7, 41–51.

Chopra, A.K., Goel, R.K., 2002. A modal pushover analysis procedure for estimating seismic demands for buildings. Earthq. Eng. Struct. Dyn. 31, 561–582.

Chopra, A.K., Goel, R.K., Chintanapakdee, C., 2004. Evaluation of a modified MPA procedure assuming higher modes as elastic to estimate seismic demands. Earthq. Spectra 20, 757–778.

Comartin, C.D., 1996. Seismic evaluation and retrofit of concrete buildings. Seismic Safety Commission, State of California.

D’Ambrisi, A., De Stefano, M., Tanganelli, M., 2009. Use of pushover analysis for predicting seismic response of irregular buildings: a case study. J. Earthq. Eng. 13, 1089–1100.

DesRoches, R., Choi, E., Leon, R.T., Dyke, S.J., Aschheim, M., 2004. Seismic response of multiple span steel bridges in central and southeastern United States. I: As built. J. Bridge Eng. 9, 464–472.

Di Sarno, L., Wyatt, T., 2006. High rise steel buildings under wind loads. Presented at the XI International Conference on Metal Structures (ICMS-2006), Taylor &Francis Group, pp. 362–364.

Elnashai, A.S., Di Sarno, L., 2015. Fundamentals of earthquake engineering: from source to fragility. John Wiley & Sons.

Ferry, M., Meghraoui, M., Abou Karaki, N., Al-Taj, M., Khalil, L., 2011. Episodic Behavior of the Jordan Valley Section of the Dead Sea Fault Inferred from a 14-ka-Long Integrated Catalog of Large EarthquakesEpisodic Behavior of the Jordan Valley Section of the Dead Sea Fault. Bull. Seismol. Soc. Am. 101, 39–67.

Floren, A., Mohammadi, J., 2001. Performance-based design approach in seismic analysis of bridges. J. Bridge Eng. 6, 37–45.

Frosch, R.J., Kreger, M.E., Talbott, A.M., 2009. Earthquake resistance of integral abutment bridges.

Fu, X., Gu, L., Yang, X., Yu, W., Chen, X., 2005. Structural design and research on Beijing Olympic National Swimming Center. Spat. Struct. 11, 14–21.

Garfunkel, Z., 2014. Lateral motion and deformation along the Dead Sea transform, in: Dead Sea Transform Fault System: Reviews. Springer, pp. 109–150.

Hartman, G., Niemi, T.M., Tibor, G., Ben-Avraham, Z., Al-Zoubi, A., Makovsky, Y., Akawwi, E., Abueladas, A., Al-Ruzouq, R., 2014. Quaternary tectonic evolution of the northern gulf of elat/aqaba along the Dead Sea transform. J. Geophys. Res. Solid Earth 119, 9183–9205.

Huang, K., Kuang, J.S., 2010. On the applicability of pushover analysis for seismic evaluation of medium-and high-rise buildings. Struct. Des. Tall Spec. Build. 19, 573–588.

Itani, A.M., Bruneau, M., Carden, L., Buckle, I.G., 2004. Seismic behavior of steel girder bridge superstructures. J. Bridge Eng. 9, 243–249.

Kim, S., D’Amore, E., 1999. Push-over analysis procedure in earthquake engineering. Earthq. Spectra 15, 417–434.

Klinger, Y., Le Béon, M., Al-Qaryouti, M., 2015. 5000 yr of paleoseismicity along the southern Dead Sea fault. Geophys. J. Int. 202, 313–327.

Le Béon, M., Klinger, Y., Mériaux, A., Al-Qaryouti, M., Finkel, R.C., Mayyas, O., Tapponnier, P., 2012. Quaternary morphotectonic mapping of the Wadi Araba and implications for the tectonic activity of the southern Dead Sea fault. Tectonics 31.

Machida, A., Khairy Hassan, A., 2000. Effect of shear reinforcement on failure mode of RC bridge piers subjected to strong earthquake motions. Presented at the Proceedings of the 12th World Conference on Earthquake Engineering (WCEE), Auckland.

Mander, J.B., Kim, D., Chen, S., Premus, G., 1996. Response of steel bridge bearings to reversed cyclic loading.

Moghaddam, H., Hajirasouliha, I., 2006. An investigation on the accuracy of pushover analysis for estimating the seismic deformation of braced steel frames. J. Constr. Steel Res. 62, 343–351.

Nguyen, P.-C., Kim, S.-E., 2014. Nonlinear inelastic time-history analysis of three-dimensional semi-rigid steel frames. J. Constr. Steel Res. 101, 192–206.

NYSDOT (2004). Seismic Vulnerability Manual. New York State Department of Transportation, New York, NY., n.d.

Pan, P., Ohsaki, M., 2006. Nonlinear multimadal pushover analysis method for spatial structures. Presented at the International Symposium on New Olympic, New Shell and Spatial Structures.

Pan, Y., Agrawal, A.K., Ghosn, M., 2007. Seismic fragility of continuous steel highway bridges in New York State. J. Bridge Eng. 12, 689–699.

Pan, Y., Agrawal, A.K., Ghosn, M., Alampalli, S., 2010a. Seismic fragility of multispan simply supported steel highway bridges in New York State. I: Bridge modeling, parametric analysis, and retrofit design. J. Bridge Eng. 15, 448–461.

Pan, Y., Agrawal, A.K., Ghosn, M., Alampalli, S., 2010b. Seismic fragility of multispan simply supported steel highway bridges in New York State. II: Fragility analysis, fragility curves, and fragility surfaces. J. Bridge Eng. 15, 462–472.

Paraskeva, T.S., Kappos, A., Sextos, A., 2006. Extension of modal pushover analysis to seismic assessment of bridges. Earthq. Eng. Struct. Dyn. 35, 1269–1293.

Sadeh, M., Hamiel, Y., Ziv, A., Bock, Y., Fang, P., Wdowinski, S., 2012. Crustal deformation along the Dead Sea Transform and the Carmel Fault inferred from 12 years of GPS measurements. J. Geophys. Res. Solid Earth 117.

Salamon, A., Rockwell, T., Ward, S.N., Guidoboni, E., Comastri, A., 2007. Tsunami hazard evaluation of the eastern Mediterranean: historical analysis and selected modeling. Bull. Seismol. Soc. Am. 97, 705–724.

Satish, B.J.N., Reddy, B.A., Venkatesh, C., Reddy, K.H.K., Bellum, R.R., 2022. Seismic performance of a truss bridge with different substructure configurations. Innov. Infrastruct. Solut. 7, 1–12.

Schattner, U., Ben-Avraham, Z., 2007. Transform margin of the northern Levant, eastern Mediterranean: From formation to reactivation. Tectonics 26.

Schattner, U., Weinberger, R., 2008. A mid-Pleistocene deformation transition in the Hula basin, northern Israel: Implications for the tectonic evolution of the Dead Sea Fault. Geochem. Geophys. Geosystems 9.

Sneh, A., Weinberger, R., 2014. Major structures of Israel and Environs, scale 1: 500,000. Isr. Geol. Surv. Jerus.

Walls, S.M., 2004. FEMA 356 Prestandard and Commentary for the Seismic Rehabilitation of Buildings, ASCE for the Federal Emergency Management Agency, Washington, DC, November 2000. Forghani R., Totoev YZ y Kanjanabootra S., Experimental investigation of the water penetration through semi interlocking masonry (SIM) walls, Proc. Annual Meeting of Architectural Institute of Japan, Kobe, Japan, September 2014, pp. 889-890. Mason. Soc. J. 25, 41–52.

Weinberger, R., Gross, M.R., Sneh, A., 2009. Evolving deformation along a transform plate boundary: Example from the Dead Sea Fault in northern Israel. Tectonics 28.

Yin, Y., Wang, S., Fang, Z., 2019. Verification of pushover analysis for a long-span steel truss structure. J. Vibroengineering 21, 420–430.

Zaslavsky, Y., Rabinovich, M., Perelman, N., Avirav, V., 2009. Seismic hazard maps in terms of spectral acceleration at period of 0.2 sec and 1 sec for design response spectrum (tow-point method) in the new version of the Israel building code (SI 413). Natl. Steer. Comm. Earthq. Prep. Rep. No 522474 9, 36.

Zatar, W., Harik, I.E., Yuan, P., Choo, C.C., 2006. Preliminary seismic evaluation and ranking of bridges along I-24 in Western Kentucky. University of Kentucky Transportation Center.

ZHANG, W., QIAN, J., 2010. Application of pushover analysis in estimating seismic demands for large-span spatial structure. Presented at the Symposium of the International Association for Shell and Spatial Structures (50th. 2009. Valencia). Evolution and Trends

in Design, Analysis and Construction of Shell and Spatial Structures: Proceedings, Editorial Universitat Politècnica de València.

Zohar, M., Salamon, A., Rubin, R., 2016. Reappraised list of historical earthquakes that affected Israel and its close surroundings. J. Seismol. 20, 971–985.